



UPPSALA
UNIVERSITET

*Digital Comprehensive Summaries of Uppsala Dissertations
from the Faculty of Science and Technology 561*

Free molecular and metal clusters studied by synchrotron radiation based electron spectroscopy

ALDANA ROSSO



ACTA
UNIVERSITATIS
UPSALIENSIS
UPPSALA
2008

ISSN 1651-6214
ISBN 978-91-554-7307-5
urn:nbn:se:uu:diva-9323

Dissertation presented at Uppsala University to be publicly examined in Högssalen, Ångströmlaboratoriet, Lägerhyddsvägen 1, Uppsala, Thursday, November 13, 2008 at 13:15 for the degree of Doctor of Philosophy. The examination will be conducted in English.

Abstract

Rosso, A. 2008. Free molecular and metal clusters studied by synchrotron radiation based electron spectroscopy. Acta Universitatis Upsaliensis. *Digital Comprehensive Summaries of Uppsala Dissertations from the Faculty of Science and Technology* 561. 66 pp. Uppsala. ISBN 978-91-554-7307-5.

The main purpose of this Thesis is the experimental characterization of the electronic and geometric structures of objects called clusters. A cluster consists of a finite group of bound atoms or molecules. Due to its finite size, it may present completely different properties than those of the isolated atom and the bulk. The clusters studied in this work are constituted by rare-gas atoms, organic molecules, and metal atoms. Intense cluster beams were created using either an adiabatic expansion source or a gas-aggregation source, and investigated by means of synchrotron radiation based photoelectron spectroscopy.

The reports presented in this Thesis may be divided into three parts. The first one deals with results concerning homogeneous molecular clusters (benzene- and methyl-related clusters) highlighting how molecular properties, such as dipole moment and polarizability, influence the cluster structure. The second part focuses on studies of solvation processes in clusters. In particular, the adsorption of polar molecules on rare-gas clusters is studied. It is shown that the doping method, i.e. the technique used to expose clusters to molecules, and the fraction of polar molecules are important factors in determining the location of the molecules in the clusters. Finally, a summary of investigations performed on metal clusters is presented. The applicability of solid state models to analyse the cluster spectra is considered, and the differences between the atomic, cluster and solid electronic structures are discussed.

Keywords: nanoparticles, free clusters, molecular clusters, metal clusters, photoelectron spectroscopy, synchrotron radiation, local structure, core level spectroscopy, auger spectroscopy, heterogeneous clusters, nucleation, bromomethane, chloromethane, benzene, bromobenzene, chlorobenzene, potassium, sodium, simple metals

Aldana Rosso, Department of Physics and Materials Science, Ångströmlaboratoriet, Lägerhyddsv. 1, Box 530, Uppsala University, SE-75121 Uppsala, Sweden

© Aldana Rosso 2008

ISSN 1651-6214

ISBN 978-91-554-7307-5

urn:nbn:se:uu:diva-9323 (<http://urn.kb.se/resolve?urn=urn:nbn:se:uu:diva-9323>)

There are...Agents in Nature able to make the particles of Bodies stick together by very strong Attractions...And it is the Business of experimental Philosophy to find them out.
I. Newton, Query 31 in “Opticks”

List of Publications

This Thesis is based on the following papers, which are referred to in the text by their Roman numerals.

- I *First measurement of a size-dependent chemical shift in the C 1s x-ray photoelectron spectrum of large benzene clusters*
A. Rosso, S. E. Canton, S. Svensson, M. Tchapyguine, O. Björneholm, and G. Öhrwall
Submitted to J. Phys. B: At. Mol. Opt. Phys., (2008).

- II *The role of molecular polarity in cluster local structure studied by photoelectron spectroscopy*
A. Rosso, T. Rander, H. Bergersen, A. Lindblad, M. Lundwall, S. Svensson, M. Tchapyguine, G. Öhrwall, L. J. Sæthre, and O. Björneholm
Chem. Phys. Lett. **435**(1-3), 79 (2007).

- III *Synchrotron radiation study of chloromethane clusters: Effects of polarizability and dipole moment on core level chemical shifts*
A. Rosso, A. Lindblad, M. Lundwall, T. Rander, S. Svensson, M. Tchapyguine, G. Öhrwall, and O. Björneholm
J. Chem. Phys. **127**(2), 024302 (2007).

- IV *XPS studies of the substituent effect in clusters of aromatic molecules*
A. Rosso, S. E. Canton, S. Svensson, O. Björneholm, M. Tchapyguine, and G. Öhrwall
In manuscript, (2008).

- V *Adsorption of polar molecules on krypton clusters*
A. Rosso, W. Pokapanich, G. Öhrwall, S. Svensson, O. Björneholm, and M. Tchapyguine
J. Chem. Phys. **127**(8), 084313 (2007).

- VI *Adsorption of chloromethane molecules on free argon clusters*
A. Rosso, G. Öhrwall, M. Tchapyguine, S. Svensson, T. Rander, M. Lundwall, A. Lindblad, and O. Björneholm
J. Phys. B: At. Mol. Opt. Phys. **41**(8), 085102 (2008).

- VII *Photoelectron spectroscopy study of free potassium clusters: Core-level lines and plasmon satellites*
A. Rosso, G. Öhrwall, I. L. Bradeanu, S. Svensson, O. Björneholm, and M. Tchapyguine
Phys. Rev. A **77**(4), 043202 (2008).
- VIII *The valence band of free K clusters studied by photoelectron and Auger spectroscopies*
A. Rosso, G. Öhrwall, S. E. Canton, S. Legendre, I. L. Bradeanu, S. Svensson, O. Björneholm, and M. Tchapyguine
Submitted to Eur. Phys. J. D (2008).
- IX *Free nanoscale sodium clusters studied by core-level photoelectron spectroscopy*
S. Peredkov, G. Öhrwall, J. Schulz, M. Lundwall, T. Rander, A. Lindblad, H. Bergersen, A. Rosso, W. Pokapanich, N. Mårtensson, S. Svensson, S. L. Sorensen, O. Björneholm, and M. Tchapyguine
Phys. Rev. B **75**(23), 235407 (2007).
- X *Size determination of free metal clusters by core-level photoemission from different initial charge states*
S. Peredkov, S. L. Sorensen, A. Rosso, G. Öhrwall, M. Lundwall, T. Rander, A. Lindblad, H. Bergersen, W. Pokapanich, S. Svensson, O. Björneholm, N. Mårtensson, and M. Tchapyguine
Phys. Rev. B **76**(8), 081402(R) (2007).
- XI *Direct observation of the non-supported metal nanoparticle electron density of states by X-ray photoelectron spectroscopy*
M. Tchapyguine, S. Peredkov, A. Rosso, J. Schulz, G. Öhrwall, M. Lundwall, T. Rander, A. Lindblad, H. Bergersen, W. Pokapanich, S. Svensson, S. L. Sorensen, N. Mårtensson, and O. Björneholm
Eur. Phys. J. D **45**(2), 295 (2007).
- XII *Absolute core-level binding energy shifts between atom and solid: The Born-Haber cycle revisited for free nanoscale metal clusters*
M. Tchapyguine, S. Peredkov, A. Rosso, I. Bradeanu, G. Öhrwall, S. Legendre, S. L. Sorensen, N. Mårtensson, S. Svensson, and O. Björneholm
J. Electron Spectrosc. Rel. Phenom. doi:10.1016/j.elspec.2008.05.001 (2008).

Reprints were made with permission from the publishers.

Other Publications

In addition, I have been involved in the following works.

- *Crystal structure of pure ZrO_2 nanopowders*
D. Lamas, A. M. Rosso, M. Suarez Anzorena, A. Fernández, M. G. Bellino, M. D. Cabezas, N. E. Walsøe de Reca, and A. F. Craievich
Scripta Mater. **55**(6), 553 (2006).
- *Localized versus delocalized excitations just above the 3d threshold in krypton clusters studied by Auger electron spectroscopy*
M. Tchapyguine, A. Kivimaki, S. Peredkov, S. L. Sorensen, G. Öhrwall, J. Schulz, M. Lundwall, T. Rander, A. Lindblad, A. Rosso, S. Svensson, N. Mårtensson, and O. Björneholm
J. Chem. Phys. **127**(12), 12431 (2007).
- *Auger electron spectroscopy as a probe of the solution of aqueous ions*
W. Pokapanich, H. Bergersen, I. L. Bradeanu, R. R. T. Marinho, A. Lindblad, S. Legendre, A. Rosso, S. Svensson, O. Björneholm, M. Tchapyguine, G. Öhrwall, N. V. Kryzhevoi, and L. S. Cederbaum
In manuscript, (2008).

Comments on my own participation

Experimental physics has many facets including development and maintenance of equipment, measurements, analysis and presentation of data. The work summarized in this Thesis is the result of team-work. Consequently, my contribution to the papers has varied and it is indicated by the position of my name in the author list. For the papers in which I am the first author, I have been the main responsible for planning of the measurements, analysing the data, and writing the manuscripts. For the other reports, my contribution has consisted in taking part in the experiments at the beamline and, in a more limited fashion, in discussions regarding the physics therein.

Contents

List of Publications	5
Comments on my own participation	8
1 Populärvetenskaplig sammanfattning	13
1.1 Klusterfysik	13
1.2 Elektronspektroskopi	13
1.3 Nya resultat	14
2 Introduction	17
3 Clusters	21
3.1 Rare-gas clusters	21
3.1.1 Rare-gas cluster structures	22
3.2 Molecular clusters	23
3.2.1 Dispersion interactions	23
3.2.2 Dipole-dipole interactions	23
3.2.3 Induction forces	24
3.2.4 Comparison of intermolecular forces	25
3.3 Heterogeneous clusters	25
3.3.1 Geometry of heterogeneous clusters	26
3.4 Metal clusters	26
3.4.1 Metal cluster geometric structures	27
3.4.2 The metal-insulator transition	27
4 Experimental techniques	29
4.1 Cluster sources	29
4.1.1 Homogeneous cluster production	29
4.1.2 Heterogeneous cluster production	30
4.1.3 Cluster size	30
4.2 Photoelectron spectroscopy	31
4.2.1 Chemical shift	33
4.2.2 Spin-orbit splitting and exchange splitting	34
4.2.3 Core and valence level photoelectron spectra of clusters	35
4.2.4 Auger spectroscopy	36
4.2.5 Analysis of the CVV Auger spectrum of metal clusters	37
4.2.6 Angular distribution of photoelectrons	39
4.3 Experimental set-up	39
5 Results	41
5.1 Homogeneous molecular clusters: Papers I–IV	41
5.1.1 Van der Waals molecular clusters (Paper I)	42

5.1.2	The effects of polarizability and dipole moment in the cluster structure (Papers II–IV)	44
5.2	Heterogeneous molecular clusters: Papers V and VI	47
5.3	Metal clusters: Papers VII–XII	48
5.3.1	Valence band	49
5.3.2	Core levels	49
5.3.3	Estimation of the size of metal clusters	51
5.3.4	CVV Auger spectra of alkali metal clusters	52
5.3.5	The Born-Haber cycle applied to metal clusters	54
6	Summary and outlook	57
	Acknowledgements	59
	Bibliography	61

1. Populärvetenskaplig sammanfattning

1.1 Klusterfysik

Dagens Sverige är ett industriellt land. Jordbruket var mycket viktigt för landets ekonomi förra seklet men nu anställer det bara 2 % av den aktiva befolkningen. Den svenska exportsektorn var baserad på naturella resurser som skog, järn and vatten. Efter mitten av 1990 talet har bl.a. IT och kommunikationsteknologi tagit över det traditionella näringslivet. Detta beror till stor del på att Sverige har satsat på forskning på nya metoder och material som är optimerade för dagens och framtidens teknologi. När elektroniska komponenter blir små (≈ 0.000000001 meter) förändras deras egenskaper, dvs. materialens egenskaper är beroende på antalet atomer. Det betyder att forskarna måste förstå varför atomer sitter som de gör i fasta material för att tillverka nya föremål med de egenskaper industrin behöver. Här kommer klusterforskning in. Klusterfysik är ett ämne inom fysik som studerar hur materialens storlek, dvs. hur många atomer/molekyler materialen innehåller, påverkar deras egenskaper. Ett kluster är en grupp av atomer eller molekyler som har från två till miljontals atomer/molekyler. Klusterforskning kan ge kännedom om gränslandet mellan enskilda atomer och fasta material. Kluster tillverkas av olika material och i olika storlek. De mest studerade är kluster av ädelgaser, framför allt för att de är enkla att producera. Ädelgasklustren används för att utveckla teorimodeller. Metallkluster är intressanta på grund av potentiella applikationer inom datorindustrin. Molekylära kluster används för att tillverka nya mediciner och inom kemiska tillämpningar.

Eftersom kluster är väldigt små sitter en stor del av de ingående atomerna eller molekylerna i ytan. Klusters egenskaper påverkas därför starkt av miljön omkring dem. På grund av detta föredrar många forskare att jobba med fria kluster. Fria kluster finns exempelvis i atmosfären. Men kluster kan också vara fästa till något annat material, som metallklustren som sitter i elektroniska komponenter.

1.2 Elektronspektroskopi

Inom klusterfysik är man intresserad av hur atomer sitter ihop. Flera atomer kan bindas ihop genom att dela elektroner med varandra och beroende på hur många atomer som är involverade kan de bygga molekyler, kluster, vätskor eller fasta material. Elektronspektroskopi är en lämplig metod att undersöka

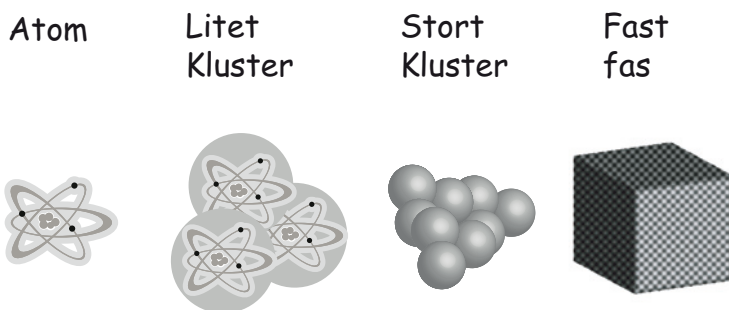


Figure 1.1: Från atom, via små och stora kluster, till den nästan oändliga fasta fasen.

fria kluster. Forskarna använder då ljus för att slå ut elektroner från klustren. Forskarna kan välja ljusets (strålningens) energi och därmed kan de skilja på elektroner som är löst bundna, då det behövs lite energi för att slå ut dem, och elektroner som är hårt bundna, då det behövs mer energi. Genom att använda spektroskopi för att mäta hur hårt bundna alla elektronerna i materialet är, och genom att jämföra med teorimodeller kan sedan forskarna komma fram till hur klustrens struktur ser ut. Forskarna brukar bestråla kluster med allt ifrån ultraviolett strålning till röntgenstrålning för att studera de olika hårt bundna elektronerna. Maskinen som levererar lämplig strålning med olika energi kallas synkrotron.

1.3 Nya resultat

Här presenteras resultaten från undersökningar av fria ädelgas-, metall- och molekykluster. Alla experimenten gjordes på den nationella svenska synkrotronljusanläggningen MAX-lab i Lund. Vi blandade polära molekyler och ädelgaser för att skapa mixkluster. Vi tillverkade ädelgaskluster och lade därefter på lager av molekyler på klustren. Hur molekyllerna sitter är beroende på många faktorer bl.a. klustrens storlek och antalet molekyler. Vi kom fram till att molekyllerna framför allt satte sig på ytan och ädelgasatomerna befann sig inuti. Sådana resultat är viktiga eftersom man använder kluster för att påverka eller starta kemiska reaktioner (katalys). Vi gjorde också oblandade molekyllära kluster av klormetan eller brommetan, vilka båda är molekyler som bidrar till växthuseffekten. Vi studerade bensen- och brombensen- och klorbensenkluster, som används inom läkemedelindustri. Deras bindningsegenskaper liknar många biologiska molekyler som DNA. Där har vi också presenterat sannolika klusterstrukturer. Slutligen har vi

studerat metallkluster av bl.a. kadmium. Experimenten visade att våra kluster av endast ett par tusen atomer redan visade många likheter med fast kadmium med ett nästan oändligt antal atomer.

2. Introduction

The main purpose of this Thesis is the experimental characterization of the electronic and geometric structures of objects called *clusters*. A cluster consists of a finite group of bound atoms or molecules. Due to its finite size, it may present completely different properties than those of the isolated atom and the bulk. The clusters studied in this work are constituted by rare-gas atoms, organic molecules, and metal atoms. In order to study their bonding, it is necessary to consider the electromagnetic interactions. The main forces between atoms/molecules are usually classified into three categories¹ according to their dependence on the interatomic distance: the purely electrostatic forces arising from the Coulomb forces between charges, the polarization forces, which appear when a dipole moment is induced in atoms and molecules by an external electric field, and the quantum mechanical forces, which cause, for example, the covalent bonding and the exchange interaction. Figure 2.1 schematically shows some of the above mentioned interactions.

In order to investigate the cluster electronic structure, it is desirable to use experimental methods that provide direct information about the distribution of electrons. Photoelectron spectroscopy is a technique that allows to probe specific orbitals. It is especially sensitive to surfaces, which is an advantage for clusters since a large fraction of the constituent atoms are located on the surface. This method consists in exposing the clusters to a radiation source with photons of higher energy than the binding energy of the level of interest. Electrons from this level are ejected from the sample and further detected. An analysis of the kinetic energy of these free electrons called photoelectrons gives the opportunity to deduce the electronic structure of the sample. In order to interpret the spectrum it is necessary to model the interaction between the photons and the electrons. The studies presented in this Thesis are mainly related to the investigation of the core or inner-shell orbitals, which are almost unperturbed when the atoms form molecules or clusters. Therefore, the formalisms already developed for atoms and molecules are used to study the core-ionization process in clusters. Even in these cases, a complete description of this interaction is extremely complicated. However, some approximations can be applied to make this problem treatable.

Since the nucleus is much heavier than the electrons we may make the approximation that, from the electrons' perspective, the nucleus is fixed². Therefore, it is possible to decouple the electronic and nuclear motions in

¹Magnetic interactions are much weaker than the above mentioned forces for the compounds studied in this Thesis.

²The mass of an electron is a factor of about 2000 less than the mass of a proton (or neutron)

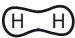
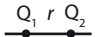
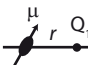


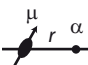
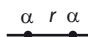
Type of interaction		Interaction Energy
covalent, metallic	 H_2	short range
charge- charge		Coulomb energy $Q_1 Q_2 / r$
charge- dipole		Fixed dipole: $-Q\mu/r^2$ Rotating dipole: $-Q^2\mu^2/kTr^4$
dipole- dipole		Fixed dipole: $\mu_1\mu_2/r^3$ Rotating dipole: $-\mu_1^2\mu_2^2/kTr^6$
charge- non-polar		$-Q^2\alpha/r^4$
dipole- non-polar		Fixed dipole: $-\mu^2\alpha/r^6$ Rotating dipole: $-\mu^2\alpha/r^6$
non-polar- non-polar		London dispersion energy $-\alpha^2/r^6$

Figure 2.1: Common types of interactions between molecules, ions and atoms in vacuum. Q is the electric charge, μ is the dipole moment, α is the polarizability, k is the Boltzmann constant, T is the temperature, and r is the distance between the interacting atoms/molecules [1].

the Schrödinger equation. This model is called the Born-Oppenheimer approximation. The interaction between the atoms and the photons is simplified if the wavelength of the radiation is large compared to the size of the atoms³. Then, the variation of the radiation field across the molecules can be neglected (dipole approximation). Within these assumptions, methods developed for interpreting molecular and solid spectra have been applied to the study of cluster core-level spectra.

This Thesis is organized in the following way. Chapter 3 presents an introduction to the main characteristics of clusters. Chapter 4 is devoted to the description of the equipment and the investigation techniques used. Chapter 5 summarizes the main results obtained for homogeneous and heterogeneous molecular clusters and metal clusters. Finally, a summary and outlook are presented in Chapter 6.

³The typical size of an atom is $\approx 1 \cdot 10^{-10}$ m and the wavelength of soft x-rays is $\approx 3 \cdot 10^{-9}$ m

The research discussed in this Thesis is further described in Papers I–XII. Papers I–IV deal with results concerning homogeneous molecular clusters, highlighting how molecular properties, such as dipole moment and polarizability, influence the cluster structure. The adsorption of polar molecules on rare-gas clusters is discussed in Papers V and VI. There it is shown that the doping method, *i.e.* the technique used to expose clusters to molecules, and the fraction of polar molecules are important factors in determining the location of the molecules in the clusters. Papers VII–XII summarize the investigation of metal clusters by electron spectroscopies. The applicability of solid state models to analyse the cluster spectra is considered. One of the main points of these Papers is the comparison between the electronic structure of the isolated atom, the cluster, and the infinite solid.

3. Clusters

In physics, the term clusters refers to an aggregate of a finite number of bound atoms and/or molecules ranging from two up to million atoms. This is an interesting size regime because it lies in between the gas phase and the solid phase. Clusters can present different properties from those of molecules/atoms and condensed matter. They are classified according to the type of constituent monomers, and the nature of the bonding. In this chapter, the main characteristics of rare-gas, molecular and metal clusters are discussed.

3.1 Rare-gas clusters

Rare-gas clusters were the first to be studied because they are relatively easy to produce and to simulate due to their closed shell structure [2]. The attraction between the atoms in the clusters is caused by (London) dispersion forces, which are the dominant part of the van der Waals forces (vdW). The forces are caused by fluctuations of the electronic density that create instantaneous multipoles which attract/repel each others. These forces become stronger as the atom (or molecule) becomes larger because the polarizability, which characterises the tendency of a charge distribution to be distorted by an external electric field, increases with the size of the electron cloud. The vdW forces are long-range forces that can be, under certain circumstances, effective from large distances (greater than 10 nm) down to interatomic spacing (0.2 nm) [1]. The vdW interaction brings the atoms/molecules together. The electrostatic repulsive forces and the Pauli principle set a limit for the compressibility of matter.

The potential caused by the attractive dispersion forces and the repulsive forces between pair of atoms/molecules is usually modelled by the Lennard-Jones pair potential energy function (LJ):

$$V^{LJ} = 4\epsilon \left\{ \left(\frac{\sigma}{r} \right)^{12} - \left(\frac{\sigma}{r} \right)^6 \right\} \quad (3.1)$$

where $-\epsilon$ is the minimum of the potential energy, r is the internuclear distance between the atoms, and σ is the internuclear length parameter for which $V(\sigma) = 0$ [3]. The choice of the exponent 6 in Eq. (3.1) is consistent with the lowest exponent of the London dispersion forces between spherical nonpolar atoms/molecules (see Fig. 2.1), while the coefficient 12 is rather arbitrary and is chosen for simplicity [3]. This function can be also used to model the interaction between rare-gas atoms in a cluster because even though the forces

between three or more rare-gas atoms are not additive, many-body effects in rare-gas clusters are generally small and can be neglected [2]. Table 3.1 shows the LJ parameters and the boiling point for argon and krypton [2]. An estimation of the temperature below which dimers (clusters constituted by two atoms/molecules) can be formed is given by $T_d = \varepsilon/k$, where k is the Boltzmann constant. Krypton has higher dimer formation temperature than argon because the dispersion forces in the former are stronger due to its higher polarizability. Due to the weak nature of the vdW forces, their contribution to the dimer binding energies are low. A measure of the strength of the dispersion forces in atoms (or molecules) is given by the boiling point. The stronger the dispersion forces, the more energy is required to separate the atoms, the higher the temperature required to provide this energy. Krypton has a higher boiling point than argon because the dispersion forces are stronger in krypton. The boiling point is an important factor in the choice of the experimental conditions for producing clusters (see Section 4.1).

Rare-gas	ε (meV)	σ (Å)	T_b (°C)
Ar	10.2	3.4	-185.7
Kr	13.6	3.9	-153.1

Table 3.1: *Lennard-Jones parameters ε and σ , and boiling point T_b for argon and krypton [3].*

3.1.1 Rare-gas cluster structures

Small rare-gas clusters adopt an icosahedral structure because this packing maximizes the number of nearest neighbour attractive interactions, and by that the cluster surface energy is minimized. This leads to an equilateral geometry for trimers, and a tetrahedron for clusters with four atoms. Larger clusters are built by bringing tetrahedral units together. Clusters containing a number of atoms that allows them to complete a geometric shell ($N = 13, 55, 147, 309$) are more stable. These numbers N called *magic numbers* can be predicted from calculations using the Lennard-Jones potential and have been observed experimentally. The surface coordination is greater for icosahedral than for other geometric shells based on common crystalline structures, such as fcc, hcp, and bcc. As noted, the icosahedral geometry minimizes the surface distances by shortening the radial distances, so that the repulsion forces are reduced. However, for large clusters this compression induces a mechanical stress that eventually destabilizes the icosahedral structure relative to fcc-like geometries. Thus, a phase transition occurs at a critical size (N_c) from the icosahedral structure¹ to the crystalline fcc structure. Electron diffraction

¹The five-fold symmetry of the icosahedron is incompatible with the three-dimensional periodicity in solid crystals.

studies performed on argon clusters suggested that N_c is between 800 and 1000 atoms [4].

3.2 Molecular clusters

Most molecular clusters are formed by stable molecules, which can have open or closed electronic shells. The clusters are held together by weaker intermolecular forces while within each molecule the atoms are held together by covalent bonds (the atoms within the molecule *share* their electrons). The covalent forces are of short range, typically between 0.1 and 0.2 nm (see Fig. 2.1). Covalent bonding includes many kinds of interactions, *e.g.* σ -bonding, π -bonding, etc. These bonds also possess directionality, therefore the covalent bonds determine the way the atoms will coordinate in molecules. In this case not only the vdW forces but also the intermolecular attractions cause the molecules to aggregate. In aromatic systems, the interaction created by the overlap of the p-orbitals called $\pi - \pi$ interaction plays a major role in determining the crystal structures of aromatic compounds². For instance, this interaction is of fundamental importance in fullerene structures [6]. The intermolecular forces most frequently involved in the bonding of molecular clusters are: the dispersion interactions, the dipole-dipole interactions and the induction forces.

3.2.1 Dispersion interactions

Dispersion forces (vdW) arise due to instantaneous atom-centred dipoles and are present in the bonding of all types of clusters. They are dominant in the case of homonuclear molecular clusters. Typical binding energies of molecular clusters due to dispersion forces are larger than those of rare-gas clusters since the molecules are larger and in general more polarizable. Table 3.2 shows the Lennard-Jones parameters for some molecules whose clusters have been studied in this Thesis. There it is noted that ϵ , which is an indicator of the binding energy of the dimer, is larger for molecular clusters than for the rare-gas clusters.

3.2.2 Dipole-dipole interactions

Many molecules possess a permanent electric dipole moment. For example, in the water molecule, the oxygen atom is more electronegative than the hydrogen atoms, and it attracts the hydrogen's electrons leaving one part of the molecule negatively charged relative to the other end. Thus, the molecule has a permanent dipole moment. Such molecules are called polar molecules. The dipole moment of a polar molecule μ is defined as $\mu = Q \cdot r$ where r is the dis-

²In simple aromatic crystals the VdW interaction between molecules is roughly proportional to the area of the π overlap [5]

tance between two charges $+Q$ and $-Q$. Other examples of polar molecules studied in this Thesis are CH_3Br , CH_3Cl , $\text{C}_6\text{H}_5\text{Br}$, and $\text{C}_6\text{H}_5\text{Cl}$, in which the halogen atoms are charged negatively relative to the rest of the molecule. In general, small molecules have moments of the order of 1 debye³. Hence, the dipole moments of H_2O , CH_3Br , CH_3Cl , $\text{C}_6\text{H}_5\text{Br}$, and $\text{C}_6\text{H}_5\text{Cl}$ (1.85, 1.82, 1.89, 1.70 and 1.69 D [7] respectively) are considered to be large. In the case of CH_3Br , CH_3Cl , $\text{C}_6\text{H}_5\text{Br}$, and $\text{C}_6\text{H}_5\text{Cl}$ the dipole moment is directed along the halogen-carbon axis.

When two polar molecules are close to each other, there is a tendency for the dipoles to align head-to-tail. The energy of the interaction V^{DD} between two co-linear dipoles μ_1 and μ_2 at zero temperature arranged in a head-to-tail fashion and separated by an r distance is proportional to $1/r^3$ (see Fig. 2.1). However, the thermal energy tends to misalign the dipoles and therefore, the energy is proportional to $1/r^6$. Examples of dimers bound by dipole-dipole forces are CH_3Br and CH_3Cl dimers.

In large clusters constituted by molecules with a strong dipole moment, the dipole-dipole interaction is important. Furthermore, qualitative arguments on how the electric moments can be arranged to minimize the energy of the cluster give insight into the cluster local structure. This concept has been used in the articles presented in this Thesis. In particular, the local structures of CH_3Br , CH_3Cl , $\text{C}_6\text{H}_5\text{Br}$, and $\text{C}_6\text{H}_5\text{Cl}$ clusters (Papers II–IV) are inferred by using these considerations.

Some molecules may possess higher order multipole moments, arising from the asymmetry in the electron density. For example, benzene has no dipole moment but it has a quadrupole moment. Multipole interactions are also important in determining the dimer and cluster structure, even when they are not the dominant forces. In cases where the quadrupole interaction is significant, the T-shaped geometry is generally adopted for the dimer, as it is experimentally found in benzene dimers [8; 9; 10]. Some considerations about the structure of large benzene clusters are discussed in Paper I.

3.2.3 Induction forces

All atoms and molecules are polarizable. A molecule can acquire a dipole moment in the electric field produced by its neighbours. The strength of the interaction depends on the polarizability of the molecule (see Fig. 2.1). Higher multipoles can also be induced by neighbouring molecules with a permanent charge (monopole) or higher order multipoles. Examples of this interaction are found in $\text{Kr-CH}_3\text{Cl}$ and $\text{Ar-CH}_3\text{Cl}$ clusters (Papers V and VI), in which the dipole moment of chloromethane induces a distortion in the electron density of the rare-gas atoms.

³The debye D is the CGS unit for the electrical dipole moment. It is defined as $1 \cdot 10^{-18}$ stat-coulomb centimetre. In SI units, 1 D equals approximately $3.3 \cdot 10^{-30}$ coulomb-meter.

3.2.4 Comparison of intermolecular forces

Neutral clusters are bound by vdW forces but there can also be contributions from other forces like dipole-dipole interaction depending on the nature of the molecules involved. In most cases, the largest contribution is provided by the dispersion energy. Induction energies are small unless the species are charged. In order to obtain an estimation of the strength of the intermolecular interactions the Lennard-Jones potential (Eq. (3.1)) can be used. It is worth noticing that this approximation only provides order of magnitude estimations when the molecules are polar or posses an asymmetric shape. Table 3.2 shows these coefficients for some molecules studied in this Thesis. Argon and krypton are included in Tab. 3.2 for comparison. As mentioned in Sec. 3.1, the boiling point is a macroscopic measure of the strength of the intermolecular forces. Molecules with a large dipole moment have higher boiling points than molecules with similar mass but with a smaller dipole moment.

	ϵ (meV)	σ (Å)	T_b (°C)	μ (D)	Main cluster bonding forces
Ar	10.2	3.4	-185.7	0	vdW
Kr	13.6	3.9	-153.1	0	vdW
C ₆ H ₆	19.7	4.3	80.2	0	vdW
C ₆ H ₅ Cl	20.7	4.8	131.9	1.69	vdW & D-D
C ₆ H ₅ Br			156.2	1.70	vdW & D-D
CH ₃ Br	17.6	3.5	3.6	1.82	vdW & D-D
CH ₃ Cl	17.8	3.8	-23.9	1.89	vdW & D-D

Table 3.2: Lennard-Jones coefficients ϵ and σ (Eq. (3.1)) [3; 11; 12], boiling point T_b [7], dipole moment μ [7], and main cluster bonding forces for some substances used to produce the clusters studied in this Thesis. vdW and D-D denotes van der Waals and dipole-dipole interactions respectively.

3.3 Heterogeneous clusters

Clusters have a very large fraction of their atoms/molecules located on the surface, a fact that facilitates the investigation of surface phenomena such as diffusion and chemical reactions. Furthermore, free clusters give the opportunity to study these types of processes without the complications of a substrate. Rare-gas clusters have been extensively used as host medium to investigate diffusion processes since their properties are well established. Experimental research on doped rare-gas clusters containing argon or krypton [13; 14], and neutral [15; 16; 17; 18] or negatively charged [19; 20] molecules shows that there are several factors that affect the diffusion dynamics of molecular/atomic

impurities (dopants) “in” and “on” the clusters, *e.g.* amount and size of the dopants, cluster temperature and size, and strength of the interaction between the dopant and the cluster atoms. Theoretical studies have addressed “the single dopant case” for argon host clusters [11; 21; 22] modelling the intracluster interaction between the argon atoms and the dopants using the LJ potential. However, these results are not very reliable since the LJ function (Eq. (3.1)) is not appropriate for asymmetric molecules and it neglects many body interactions. Thus, further research is needed to understand the solvation process. In Papers V and VI experimental work on doped large rare-gas clusters is presented.

3.3.1 Geometry of heterogeneous clusters

An important question regarding heterogeneous clusters is how the host cluster configuration is affected by the inclusion of other compounds. Especially intriguing is the case of polar molecules adsorbed in rare-gas clusters because their dipoles break the spherical symmetry of the forces present in the clusters. Experimental studies of a single polar molecule deposited on argon [15; 16] and krypton [16] host clusters have indicated that the impurity preferentially occupies a site in the bulk of the clusters. However, information about clusters doped with many molecules is limited. Section 5.2 summarizes the results obtained about the structure of krypton and argon clusters exposed to a large amount of chloromethane molecules using the pick-up technique.

3.4 Metal clusters

A wide variety of clusters are formed by metal atoms. Metal clusters can even contain different types of metallic atoms. Alkali metals form large clusters in which the bonding is metallic, delocalized and non-directional, involving mainly valence *s* orbitals.

The simplest theoretical framework for studying metal clusters is the Liquid Drop Model (LDM) [2] where the cluster is considered as a uniform conducting sphere. This model describes the variation with size of many cluster properties, such as ionization potential and electron affinity. For example, the cluster ionization potential has a one over *R* dependence where *R* is the cluster radius, and converges to the work function of the solid when the cluster size tends towards the macroscopic size regime. The application of the LDM is only appropriate for medium to large clusters (hundreds to thousands atoms) because size dependent properties oscillate dramatically for small clusters. Such deviations arise from quantum size effects and surface effects that are not considered in the classical LDM.

The spherical jellium model, in which a metal cluster is considered as a uniform, positively charged sphere filled with an electron gas, works well for small alkali metal clusters [2]. Within this model, the Schrödinger equation is solved numerically for an electron that moves in the sphere under an effective

potential due to the ionic cores, whose actual positions are not important⁴ [2]. This model applies only when the clusters are molten [2] and it gives an electronic shell structure for clusters with up to several thousands atoms in some cases.

3.4.1 Metal cluster geometric structures

For small metal clusters, it is believed that the icosahedral structure is the most stable one since this structure minimizes the cluster surface energy. Computational studies indicate that free Na clusters present this structure up to at least 5000 atoms [2]. Cobalt and nickel clusters would present an icosahedral structure up to hundreds of atoms [2]. When the cluster size increases, the icosahedral packing becomes energetically expensive, and a phase transition to a bulk-like crystalline structure occurs when the number of atoms exceeds a critical value. Aluminium clusters are believed to adopt an fcc-like structure (as in the bulk state) already for clusters formed by hundreds of atoms [2].

3.4.2 The metal-insulator transition

In a small metal cluster, the electron energy levels are molecular-like. As the cluster size increases, the cluster electronic structure approaches that of the solid, that is the discrete levels overlap to form electronic bands (see Fig. 3.1). The size at which the metal-insulator transition⁵ occurs is still an open issue [2]. For mercury clusters, in which the atomic $6s$ and $6p$ electronic levels overlap to form bands as the size increases, it was predicted that the transition from vdW to covalent bonding would occur at $N = 13$ where N is the number of atoms in the cluster [24]. A further transition from covalent to metallic bonding would occur at $N = 80$ [24]. These theoretical results are in agreement with experimental studies performed by Kaiser et al. [25].

Studies on the valence and core-level structures of free large metal clusters are presented in Papers VII–XII. There it is found that the clusters created in the gas-aggregation source described in Sec. 4.1 already presented a band-like electronic structure similar to that of the corresponding solids. Furthermore, for potassium clusters collective electron modes called plasmons (see Sec. 5.3.2 and Paper VII) are observed.

⁴In cases where the valence electrons are weakly bound and the ionic background responds easily to perturbations, it is valid to neglect the position of the nuclei.

⁵“The metal-insulator transition is characterized by a sudden change in electrical transport properties (conductivity) due to a reversible change from localized to itinerant behaviour of the electrons” [23].

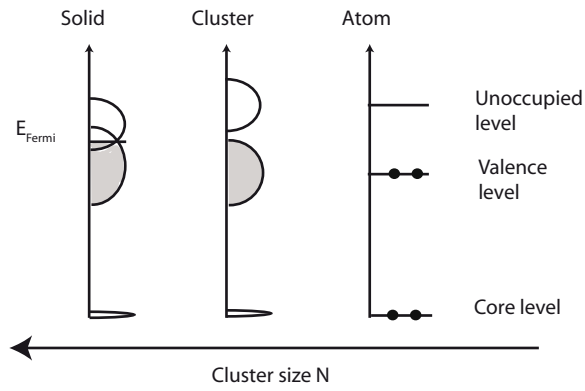


Figure 3.1: Evolution of the electronic structure from an atom to the bulk solid as a function of the cluster size N . When the cluster size increases, the bands overlap to eventually approach the electronic structure of the solid.

4. Experimental techniques

The first free nanoscale cluster sources became available in the seventies and could produce beams of rare-gas clusters [4]. Ten years later, sources able to create free metal clusters were introduced [26]. Nowadays there are several designs of cluster sources available with different degrees of sophistication [27]. The cluster sources used in the experiments presented in this Thesis are an adiabatic expansion source and a gas-aggregation source.

The clusters are investigated by means of photoelectron spectroscopy (PES) combined with synchrotron radiation. PES is an experimental method mostly developed between 1950 and 1960 that provides information regarding the chemical state, structure and properties of materials. This chapter focuses on describing the most important features of the cluster source and of the experimental set-up. A brief review of the clusterization process, the phenomena underlying the PES and its applications to the study of free clusters, is given.

4.1 Cluster sources

4.1.1 Homogeneous cluster production

Adiabatic expansion source

This technique exploits the adiabatic cooling of a stream of gas when expanding into vacuum from a small nozzle. A schematic picture of the adiabatic expansion source employed in the experiments to produce clusters is shown in Fig. 4.1. The sample in gas phase at stagnation pressure 0.1-5 bars escapes into the expansion chamber through a narrow nozzle forming a supersonic gas beam [27]. In this phase, the gas accelerates and cools down, becomes supersaturated, and condensation occurs [28]. The cluster growth stops when the density becomes too low, after a distance comparable with a few nozzle diameters from the nozzle exit. A skimmer is placed in order to extract the central part of the beam. The typical time scale for cluster growth is a fraction of milliseconds [29]. This type of source usually produces an intense cluster beam with a cluster mean size from hundreds to thousands of atoms [27]. The main factors governing the cluster size are the stagnation pressure, and the geometry and temperature of the nozzle.

Gas-aggregation source

To produce clusters of solid or liquid samples a gas-aggregation source can be employed. In this type of source the sample is vaporized into a cold inert quench gas (He or Ar). The vapour cools by collisions with the gas, and

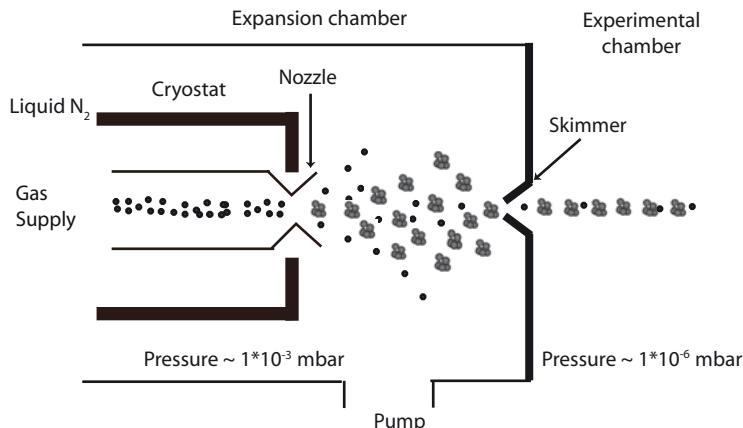


Figure 4.1: Schematic figure of the adiabatic expansion source.

aggregates into clusters. The cooling gas also sweeps the cluster into the experimental chamber. Figure 4.2 shows a sketch of the cluster source.

There are several ways to evaporate the sample. In the case of metal clusters either an oven [30] or a magnetron head [31; 30] were used to generate the vapour. For liquid samples such as benzene, chlorobenzene and bromobenzene, an oven was employed. Important factors determining the size of the clusters are the type of cooling gas and the residence time of the clusters in the aggregation zone. This type of source produces continuous cluster beams of lower intensity than those obtained from an adiabatic expansion source, but very large clusters ($> 20,000$ atoms) can be generated [27].

4.1.2 Heterogeneous cluster production

In Papers V and VI, results on heterogeneous rare-gas and molecular clusters are presented. In those experiments, argon and krypton clusters created by adiabatic expansion were exposed to a beam of molecules to create heterogeneous clusters. This method is called *doping/pick-up* and its principles are shown in Fig. 4.3.

4.1.3 Cluster size

In an adiabatic expansion source, the final cluster size and structure are given by the interplay between the experimental conditions (nozzle temperature and geometry and the stagnation conditions), the thermodynamic properties of the sample, and the stability of the electronic and geometric configurations. Establishing the mean size of free neutral clusters is a challenging problem. Hagena [32] has introduced a scaling law, in which the cluster mean size is empirically related to the stagnation conditions. This scaling law has been developed for

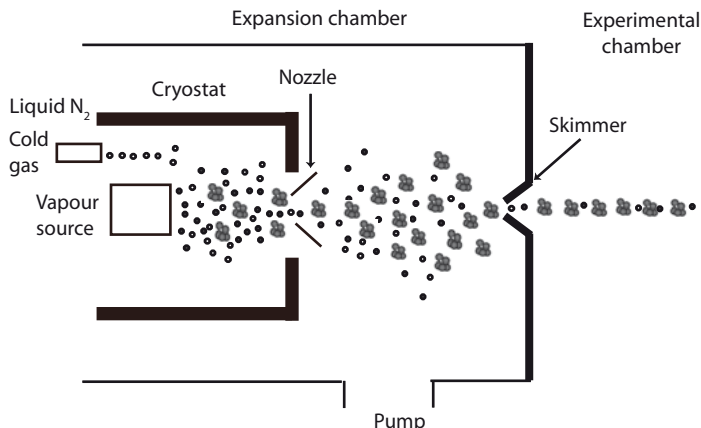


Figure 4.2: Schematic figure of the gas-aggregation source.

atomic clusters and the estimations can differ by a factor of two or more [33]. In the case of clusters created using a gas-aggregation source, their size depends on the residence time of the clusters in the aggregation zone. The observed abundances from this source are determined by collision statistics, and are smooth functions of cluster size [2].

Information regarding the cluster mean size can also be inferred from the cluster photoelectron spectrum (see Sec. 4.2) [33; 34; 35; 36; 37; 38]. For instance, in homogeneous clusters the cluster mean size can be estimated on the basis of the shape analysis of the core-level photoelectron spectra [35]. This method is used in Paper VII to estimate the mean size of potassium clusters.

In the case of metal clusters, the size can be estimated from a simple electrostatic model that relates the size and the first ionization energy of the clusters with the work function of the metal (see Sec. 5.3.3).

The cluster size of heterogeneous clusters created employing the pick-up technique are difficult to estimate. An estimation of the size of the host clusters can be performed using scaling laws [32]. However, when the dopant molecules/atoms bind to the host clusters, the cluster temperature increases, and the main cooling mechanism is the evaporation of monomers. Therefore, there is no simple way to relate the final size of the clusters with the size of the host.

4.2 Photoelectron spectroscopy

The phenomenon of photoemission was first detected by Heinrich Hertz in 1887. He noticed that a charged object lost its charge more readily when illuminated by ultraviolet light. This effect was explained by Einstein in 1905 invoking the quantum nature of the light. The first experiments in x-ray photo-

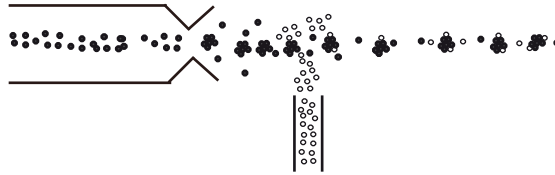


Figure 4.3: Schematic representation of the doping/pick-up method to produce heterogeneous clusters. The host clusters are created in the first stage and then exposed to a beam of molecules/atoms. The host clusters may pick up some of these molecules/atoms and form heterogeneous clusters.

electron spectroscopy (XPS) were performed at the beginning of last the century although the most important developments came during the 1950s and 1960s. Modern electron spectroscopy was pioneered by K. Siegbahn and co-workers. One of the first application of photoelectron spectroscopy to the study of molecular cluster beams was reported by Jones et. al [39] in 1978. However, this technique was not implemented to investigate free metal clusters until recently (see Ref. [40] and Papers VII–XII).

The basic experiment in photoelectron spectroscopy (PES) for gas samples, such as cluster beams, consists in exposing the gas to a flux of nearly monoenergetic radiation with mean energy $h\nu$, and then collecting the resultant photoelectrons, whose kinetic energy is described by the *photoelectric equation*,

$$E_{kin} = h\nu - E_b(k) \quad (4.1)$$

where $E_b(k)$ is the binding energy or ionization potential of the k th level (referred to vacuum), E_{kin} is the photoelectron kinetic energy, and h is the Planck constant [41].

The energy of the incoming photon can be in the ultraviolet regime (5–100 eV), in the soft x-ray regime (100–1000 eV), or in the x-ray regime (> 1000 eV). When employing ultraviolet radiation only the lowest energy electronic states of the sample are ionized. Thus, information mostly about the valence states is obtained. When the photon energy is increased, it is possible to ionize core levels. The core-level energies are unique to each element of the periodic table, since the core electrons are tightly bound to the atoms. This makes XPS an element-sensitive technique, which is a great advantage. The core levels

are discrete in binding energy. In the spectra, this gives rise to single peaks rather than bands like the valence levels. Figure 4.4 schematically shows how the photoelectron kinetic energy and electronic level in an atom are related.

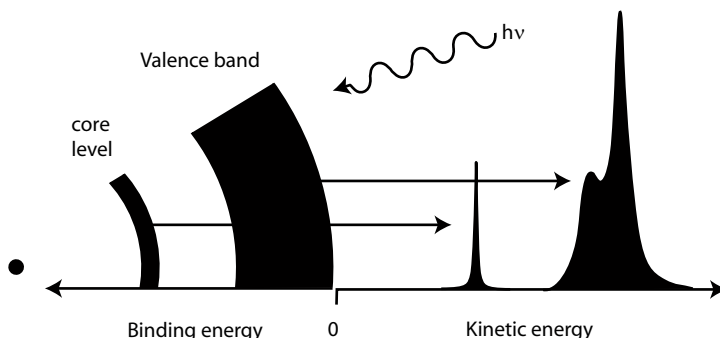


Figure 4.4: Schematic representation of the photoelectric law. The atom is ionized with a photon with energy $h\nu$. The difference between the binding energy of the electron and the energy of the photon is transferred to the ejected electron. This figure is reprinted with the kind permission of A. Lindblad [42].

For soft x-ray excitation, the escape depth of the electrons is short¹. Therefore PES is, in this case, a surface sensitive experimental probe, which is an advantage when studying clusters because a large fraction of their atoms lies on the surface.

4.2.1 Chemical shift

During the first years of photoelectron spectroscopy, a great effort was made to determine the electron binding energies in various atoms, and almost all atoms were studied in this way [43]. During this process, it was soon discovered that this energy does depend on the chemical environment of the atom studied. The change in binding energy between two different chemical forms of the same atom is denominated chemical shift. The first observation of this effect was made by Sokolowski et al. [44] in 1957, where a shift of several electron volts was registered between metallic copper and copper oxide.

Polarization screening effect

In clusters, the redistribution of the electron density around the ion depends on the cluster geometry and the polarizability of the atoms. This screening lowers the energy of the final state and, consequently the cluster peaks are shifted

¹Most of the detected photoelectrons only travel from a distance of a few Å under the surface of the sample.

relative to the molecular/atomic features towards the lower binding energy side. This effect, known as *polarization screening*, is dominant in the case of weakly-bound clusters [33]. Figure 4.5 illustrates how the cluster spectral features are shifted relative to the molecular ones. In Papers I–VI, the dominant local structure has been proposed by comparing the core-level shifts of the corresponding molecules/atoms. These results are further discussed in Sections 5.1 and 5.2.

In the case of large metal clusters, the valence electrons are completely mobile. This allows them to screen the core hole more efficiently than in molecular and rare-gas clusters.

Since all the spectra studied in this Thesis are taken in the high-energy photoelectron limit, the interaction between the photoelectron and the remaining system has been neglected (sudden-approximation).

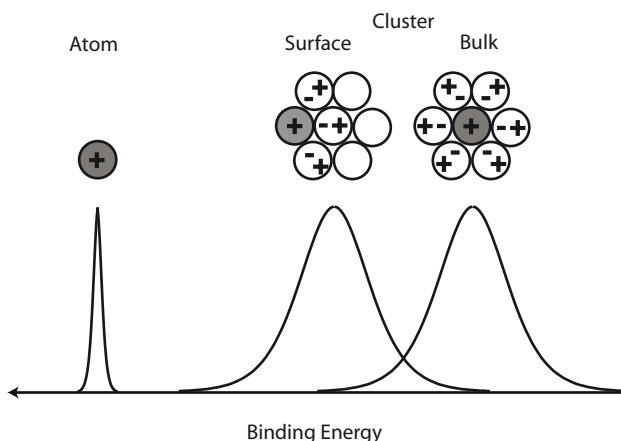


Figure 4.5: Schematic representation of the polarization screening effect in a neutral vdW or weakly-bond cluster. When a core hole is created in an atom in the cluster, the electron density of the surrounding atoms redistributes to screen the hole lowering the final state energy. Therefore, the cluster features are observed at a different binding energy than the corresponding atomic/molecular peaks.

4.2.2 Spin-orbit splitting and exchange splitting

Spin-orbit coupling occurs if an electron ejection leads to an ion with a hole in any orbital other than an s orbital [41]. In this case, the ion has an electron which spin is unpaired. This electron can have its spin and angular momenta either parallel or anti-parallel. Thus, more than one ion state is allowed and they have different binding energies. Consequently, more than one peak is observed in the spectrum.

Exchange splitting is another mechanism that has to be considered [41]. The coupling between the spin and angular momenta of the core hole and

those of the valence shell causes several final states, thus several peaks can be observed².

4.2.3 Core and valence level photoelectron spectra of clusters

The core-level spectrum in clusters

In order to be able to extract as much information as possible from the PE spectra, the photoemission process needs to be described in a mathematical way. Since the core levels are localized, it is possible to apply the lineshapes from gas phase (molecular and atomic clusters) and from solid phase (large metal clusters) to model the cluster core-level spectra.

In the case of vdW clusters, the cluster lineshape has been approximated by the convolution of a Lorentzian and a Gaussian functions. The Lorentzian width is inversely proportional to the lifetime of the core hole [41]. The Gaussian function takes into account the following mechanisms that cause broadening of the cluster features:

- variations in screening in each cluster given by differences in the coordination number,
- intermolecular vibrations,
- Doppler broadening,
- instrumental broadening,
- cluster size distribution.

As noted, in weakly bound molecular and rare-gas clusters, the atoms near the core-ionized atom would be polarized to screen the core-hole potential shifting the cluster features towards lower binding energy relative to the molecular/atomic peaks (see Section 4.2.1).

In the case of metal clusters (see Sec. 5.3.2), the core hole is neutralized by an electron which moves onto the site of the photoemission process [41]. In the screening process, the core hole produces excitations in the Fermi sea of conduction electrons. These excitations are either electron-hole pairs, which are seen as an asymmetric tail of the cluster core-level component, or collective oscillations of the system of electrons relative to the lattice ions, which show up in the spectra as sidebands [41]. The core-level peaks are described as a convolution of a Lorentzian and a singular function [41] and the resulting profile is called a Doniach-Šunjić (DS) [45]. In order to take into account those broadening effects listed above, the DS profile is convoluted with a Gaussian function.

Satellites

After the ionization, the remaining system is in an excited state. If the valence band consists of a collection of close lying discrete levels, some valence electrons can be excited by the core-hole potential. These processes are seen in the spectra as satellites, usually at higher binding energy. In some systems, for instance in simple metals, collective oscillations of the valence electrons are

²For instance, the final states after the ionization of the 1 *s* level of lithium are ¹S and ³S.

possible (plasmons), and these are observed as extra bands/peaks usually on the lower kinetic energy side of the core line.

The valence spectrum in clusters

The valence spectrum is more complicated than the core-level one. This is because the hole is created in the relaxing system, and the valence states are delocalized. A simple approach to model valence spectra of clusters has not been developed yet. However, in certain compounds like CH_3Br and CH_3Cl , whose valence levels are partially localized, an analysis similar to that of core-level spectra can be performed (see Papers II and III).

4.2.4 Auger spectroscopy

The emission of one electron after photoionization leaves the system in an excited state. There are several alternative decay paths for the excited state. In this Thesis the Auger decay, which is dominant for the light elements, is considered. In the normal Auger decay (see Fig. 4.6), the primary hole is created in a core level, and it is filled by an electron from a higher level³. The energy realised in this process is carried away by another electron. This electron is called *Auger electron*. In the case of a core-core-core (CCC) Auger transition all the levels involved are atomic-like, and in a core-valence-valence (CVV) or core-core-valence (CCV) Auger transitions at least one is from a core level, thus the energy of the Auger electron is highly characteristic of an individual atom. This means that Auger spectroscopy (AES), like XPS, is an element sensitive technique.

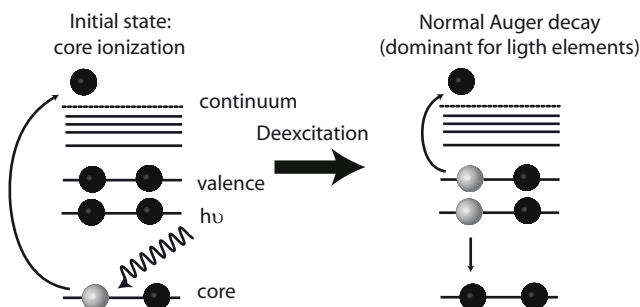


Figure 4.6: Normal Auger decay in an isolated atom.

When an atom is in a core-excited state, there is a similar decay process called Resonant Auger (RA). In this case the final state is typically singly

³Under certain conditions it is possible that the electron filling the core hole is from a level with the same quantum number n . This is a Coster-Kronig transition. If the Auger electron is also from the same core level as the hole, the transition is referred to as super Coster-Kronig.

ionized, and there are two possible decay channels: spectator and participator decays, which are illustrated in Fig. 4.7. In the first case, the excited valence electron remains in an excited orbital during the Auger decay. In the second, the excited electron takes part in the decay where one electron fills the hole and another electron is ejected. It is worth noticing that the kinetic energy of the resonant Auger electron depends on the photon energy.

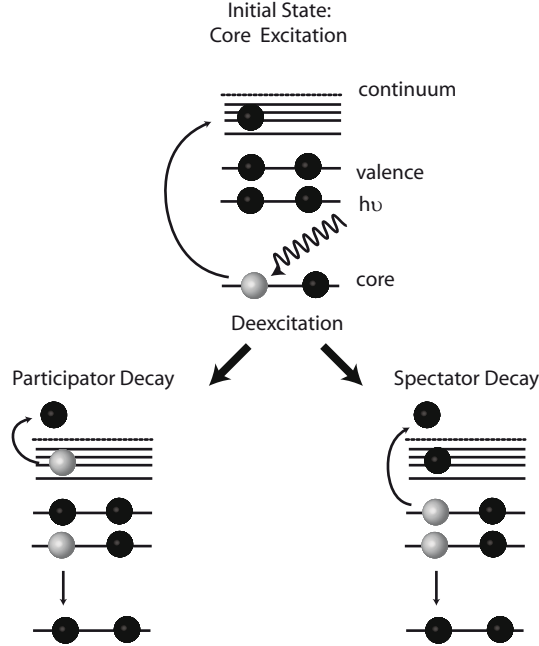


Figure 4.7: Resonant Auger decay channels in an isolated atom.

4.2.5 Analysis of the CVV Auger spectrum of metal clusters

Lander proposed a model for the Auger intensity of a CVV process in the case of metallic systems [46], which is valid when the correlation effects can be neglected [46]. The kinetic energy of the Auger electron E_{kin} is:

$$E_{kin} + (E_v - E_{k2}) = E_{k1} - E_c \quad (4.2)$$

where E_c is the core-level energy measured from the vacuum level, E_v is the Fermi energy, and E_{k1} and E_{k2} are the energies of the valence electrons involved (see Fig. 4.8) [46; 47].

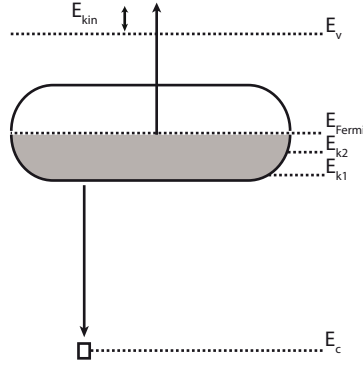


Figure 4.8: Lander model for the CVV decay. The kinetic energy of the Auger electron is equal to the sum of the kinetic energy of the valence electrons involved plus a constant according to Eq. (4.2).

The kinetic of the Auger electron E_{kin} can be also written in the following way:

$$E_{kin} = (E_{k1} + E_{k2}) - (E_v + E_c) \quad (4.3)$$

where $(E_v + E_c)$ is a constant affecting the zero energy value [46; 47]. All the Auger transitions with the same $(E_{k1} + E_{k2})$ gives the same kinetic energy of the Auger electron. Then, the lineshape is given by the sum of all the possible Auger transitions with the same energy E weighted by their probability. If it is assumed that the transition matrix elements are nearly constant across the occupied part of the valence band, and the density of states can be represented by the *free* Bloch density of states (BDOS), the Auger intensity can be written as

$$Intensity_{AES} \propto \int dx \tilde{\rho}_0(x) \tilde{\rho}_0(E - x) \quad (4.4)$$

where $\tilde{\rho}$ is the occupied BDOS [46; 47]. Equation 4.4 indicates that the Auger lineshape would be given by the self convolution of the occupied density of states. Equation 4.4 is valid within the framework of the sudden approximation (no interaction between the Auger electron and the system) with the assumption that the correlation effects are minor and the transition matrix elements are constant in the valence band. In this Thesis, Auger CVV spectra corresponding to potassium and sodium clusters are presented (see Papers VIII and IX) and the results are summarized in Sec. 5.3.4.

4.2.6 Angular distribution of photoelectrons

The angular distribution of the photoelectrons ejected from an atom relative to the direction of the incident photon beam is given by the angular momentum that they carry in order to fulfil the dipole selection rules. For linearly polarized light the angular distribution has the following form: [48]

$$I(\theta) = \frac{\theta}{4\pi} \left(1 + \frac{\beta}{2} (3 \cos^2 \theta - 1) \right) \quad (4.5)$$

where θ is the angle integrated ionization cross section and θ is the angle between the electric field vector and the direction of the emitted electron. β is an asymmetry parameter that depends on the electron wave, the element and the photon energy, and can range from -1 to 2. For example, for a pure p wave, β is 2 and $I(\theta)$ has a $\sin^2 \theta$ dependence. When $\theta = 54.7^\circ$ the angular dependence of Eq. 4.5 cancels out. This angle is called *the magic angle*. This formalism has been developed for atomic photoionization. However, Eq. 4.5 can also be used for other systems if they are completely randomly oriented [49]. Thus, Eq. 4.5 is applicable in the studies of cluster beams created in an adiabatic expansion source and in a gas-aggregation source.

4.3 Experimental set-up

The experiments discussed in this Thesis have been performed at MAX-lab, the Swedish national synchrotron radiation facility. The cluster source is attached to the beamline I411 connected to the third generation storage ring MAX II. MAX II has 1.5 GeV electron energy and a lifetime of 15-30 hours. The beamline I411 has been designed for high resolution spectroscopy on gases, liquids and condensed samples [50]. The radiation is produced by an undulator⁴, which provides photons at energies from 50 eV to 1500 eV at high flux in the order of 10^{15} photons/(sec mrad 0.1 % bandwidth) with linear polarization. The beamline is equipped with a modified Zeiss SX700 plane grating monochromator [52] and an optical focussing system. The premirror focuses the radiation from the undulator in the horizontal plane. The modified monochromator consists of three optical elements: a plane mirror, a plane diffraction grating and a focussing mirror with an elliptical shape. The photon energy is chosen by rotating the grating, which causes a dispersion of the photon beam. The monochromator directs the radiation to a torodial mirror which focuses the light in both horizontal and vertical directions toward the experimental chamber. A differential pumping stage creates a pressure difference of five orders of magnitude between the experimental chamber and the optical elements. The end station is equipped with a rotary high resolution Scienta R 4000 hemispherical electron analyser.

⁴An undulator produces periodic magnetic fields which makes the electrons wiggle with a small deviation angle. Ultra-bright and quasi-monochromatic light is then obtained because of the interference between the electromagnetic waves [51].

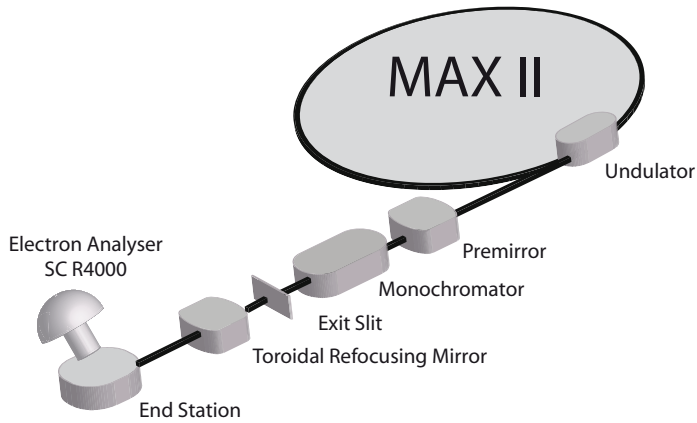


Figure 4.9: Layout of the beamline I411 at MAX-lab in Lund, Sweden. The photon beam is produced by an undulator in the MAX II ring. The premirror focuses the radiation from the undulator in the horizontal plane. The monochromator chamber consists of a plane mirror, a plane grating and a plane-elliptical mirror. The plane-elliptical mirror focuses the beam into the exit slit. The refocussing state consists of toroidal mirror which focuses the light in both horizontal and vertical directions into the end station. The total length of the beamline is 20.6 m.

5. Results: Photoelectron and Auger spectroscopies applied to the study of free clusters

Photoelectron and Auger spectroscopies are powerful tools to study clusters. They provide direct information on the intermolecular/atomic forces and on the electronic structure. Furthermore, the spectra can be used to obtain knowledge about the cluster local structure. In this chapter, a summary of the main results obtained for molecular and metal clusters probed with these methods are presented.

5.1 Homogeneous molecular clusters: Papers I–IV

The geometric and electronic structures of molecular polyatomic clusters can be different, and certainly more complex, than those of rare-gas clusters. For example while rare-gas clusters must contain thousands of atoms to reach a structure similar to the one adopted in the solid phase, some molecular clusters are believed to require only a few dozen [53; 54; 55].

Interaction in aromatic systems are of fundamental importance in physics, chemistry and biology. Benzene has been widely studied as a molecule but information about large benzene aggregates is limited. Therefore, results on large benzene clusters are presented in Sec. 5.1.1 (Paper I).

In clusters of polar molecules, there are several forces, which are not present in van der Waals clusters, that influence the cluster structure. For instance, dimers of polar molecules are expected to have a head-to-tail arrangement because of the dipole-dipole interaction. However, if the difference in polarizability of the constituent atoms is large, the head-to-head structure becomes energetically possible because the electrons of the most polarizable atom are attracted by the most electronegative atom. In order to investigate how these mechanisms affect the cluster structure, chloromethane, bromomethane, bromobenzene, and chlorobenzene clusters have been studied in Papers II–IV. These molecules present several advantages: they have a similar structure, but while chloromethane (chlorobenzene) has a larger dipole moment than bromomethane (bromobenzene), the former is more polarizable than the latter.

It is known that the substituent groups have the ability to donate or withdraw electrons, which can have significant effects on the chemical properties of a substance¹. The comparison between the results obtained for benzene-related

¹For instance, if a methyl group is added to a benzene molecule it becomes much more reactive.

clusters gives the opportunity to study the evolution of the cluster electronic structure by varying the substituent. These results are summarized in Sec. 5.1.2.

All clusters have been produced by using either an adiabatic expansion source or a gas-aggregation source, and in some cases several experimental conditions have been probed. Information about the cluster structures are obtained mostly by comparing the core- and valence-level shifts.

5.1.1 Van der Waals molecular clusters (Paper I)

Paper I reports on the local structure of large benzene clusters. Two sets of expansion conditions have been employed to create clusters, which are listed in Tab. 5.1. The results are based on the analysis of C 1s core-level and valence spectra.

P_{cg} (bar)	T_{nozzle} (°C)	T_{oven} (°C)	Cluster shift (eV)	FWHM (meV)
Series 1				
2	72.3	57.5	0.50	321
2.4	71.5	56	0.66	557
3	77	70	0.73	551
4	76	66	0.65	513
5	74	62	0.68	519
6	63.5	52	0.53	541
7	62	51	0.48	500
8	62	56	0.50	466
Series 2				
2.5	44	46	0.61	510
3	46	46.5	0.52	469
3.5	42	44	0.55	516
4	40	42	0.45	409
5	39	41	0.40	470

Table 5.1: *Experimental conditions corresponding to series 1 and 2. P_{cg} denotes the helium pressure. T_{nozzle} and T_{oven} indicate the temperatures of the nozzle and the oven respectively. The cluster shift and the full width at half maximum (FWHM) of the cluster features are also given.*

In general, the cluster formation is favoured by high density of the molecular vapour and backing pressure, and by the use of large nozzles [2]. It is observed that increasing the carrier gas pressure induces larger shifts, as expected since the cooling conditions are improved [32]. The cluster shift reaches the maximum value when the this pressure is 3 bar (see Tab. 5.1). When it becomes higher, the cluster core-level shift becomes smaller indicat-

ing that the cluster mean size decreases. The clusters lower their temperature mainly by collisions with the carrier gas and by evaporation of molecules [2]. Thus, these observations are in contrast to what is expected, since one of the main functions of the carrier gas is to improve the cooling of the clusters. If the clusters were sufficiently cold, the molecules would not evaporate and the cluster mean size, and therefore the C 1s shift, would increase. A satisfactory explanation of this behaviour requires more experimental and theoretical work.

Knowledge about the cluster geometric structure can be obtained by comparison between spectra of different aggregation states. Calculated valence and core-level shifts relative to the molecule for solid and liquid benzene [56] and experimental values for solid benzene [57; 58] are listed in Table 5.2.

Level	Gas-to-solid shift		Gas-to-liquid shift	Gas-to-cluster shift
	Experimental	Theoretical	Theoretical	Experimental
Core	2.0 [57]	1.69–2.05	1.66	0.4–0.73*
Valence	1.4 [57]	1.56–1.74	1.36	0.7*
Δ_{vc}	0.6–0.7 [58]	0.13–0.31	0.30	0.0*

Table 5.2: *Comparison between valence- and core-level shifts for benzene in gas, liquid and cluster phases. The theoretical values are taken from [56]. The cluster shifts marked with * have been obtained from spectra recorded at the same conditions. Δ_{vc} is the difference between the valence- and the core-level shifts.*

The cluster shift is different from the solid and the liquids ones, which is a strong indication that there are significant differences between the local environment of the clusters and that of the other phases. These observations are in contrast to those reported by Heenan et al. [59] and by Valente et al. [60] who stated that large benzene clusters created by adiabatic expansion presented a short range ordered structure resembling that found in crystals, which is orthorhombic with each molecule having 12 nearest neighbours [57]. The XPS measurements performed in solid samples by Riga et al. [57] could be affected by calibration errors. However, the theoretical values obtained by Ågren et al. [56] are in agreement with the experimental results obtained by Riga et al. [57]. Furthermore, the difference observed in the gas-to-solid shifts for the valence and core-level photoelectron spectra of the solid has been confirmed by x-ray emission spectroscopy (XES) measurements [58; 61; 62; 63].

Additional information about the structure is obtained from the widths of the cluster components. The cluster local structure does not seem to change with the experimental conditions, since significant variations in the widths of the cluster components are not observed (see Tab. 5.1).

5.1.2 The effects of polarizability and dipole moment in the cluster structure (Papers II–IV)

Chloromethane and bromomethane clusters (Papers II–III)

Results from the analysis of core-level spectra recorded in the C 1s and Br 3d and Cl 2p binding energy regions are displayed in Table 5.3. As seen in this work, the cluster binding energy shifts are different when either halogen or carbon atoms are core ionized. These results can be qualitatively explained using an electrostatic approach. The dipole moment would make the anti-parallel packing of the molecules the most favourable local structure in large clusters because such a configuration minimizes the electrostatic energy in the system. This arrangement would consist of CH₃ groups mainly surrounded by halogen atoms and vice versa — the halogen atoms would principally have CH₃ groups as immediate neighbours. Figure 5.1 shows a schematic representation of this intermolecular structure. It is likely that the higher electronegativity and a larger number of electrons of the halogen atoms cause stronger screening of the ionized carbon atom. On the other hand, the CH₃ groups are much less polarizable than the halogen atoms, meaning that they cannot screen the halogen ion as efficiently. Therefore, the larger cluster binding energy shift in the case of C 1s core ionization compared to the halogen case is attributed to this difference in screening. The anti-parallel packing is further supported by results of molecular dynamics simulations performed in chloromethane and bromomethane clusters formed by approximately 200 molecules [64].

Cluster	Halogen shift	Carbon shift
CH ₃ Cl	0.85 eV	1.05 eV
CH ₃ Br	0.94 eV	1.25 eV

Table 5.3: *CH₃Cl and CH₃Br cluster core-level binding energy shifts with respect to the corresponding molecular lines*

In order to compare the shifts between these systems, as above noted, two molecular properties have to be considered: the dipole moment and the polarizability. It is expected that the molecules would be more compactly packed in chloromethane than in bromomethane clusters, since the dipole moment of the former is larger than that of the latter. The halogens are in both cases largely surrounded by methyl groups, and the smaller intermolecular separation for the chloromethane case would cause a larger halogen shift for chloromethane than for bromomethane. This is in contrast to what is observed. This discrepancy can be due to other mechanisms that also play a role in the cluster shifts. For instance, the contributions from further neighbours is neglected in this model.

The valence orbitals of these molecules are partially localized in different part of the compounds which makes it possible to observe effects of the geometric configuration also in the valence region, where fingerprints of these two

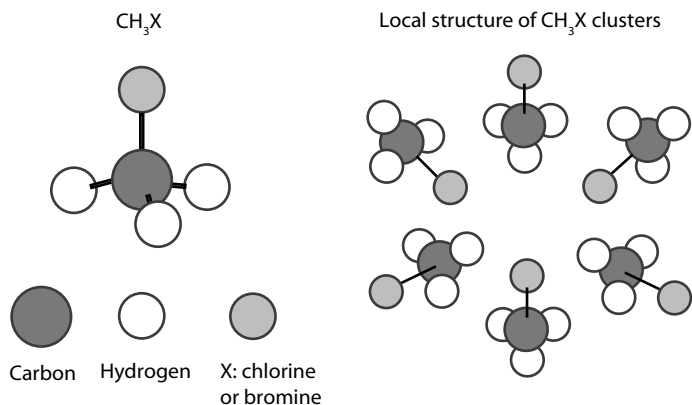


Figure 5.1: Schematic representation of a possible local structure of CH_3Br and CH_3Cl clusters. The halogen atoms are surrounded by CH_3 groups and vice versa. This type of arrangement is compatible with the dimer and the solid structures of these materials.

orbitals are well separated in binding energy [65]. In clusters, it is observed that the energy levels preserve their molecular character since the shifts of the cluster peaks vary depending on the electronic density and the degree of localization of the valence orbitals (Tab. 5.4). This difference in the shifts also indicates that the molecules are only slightly bound in the clusters by vdW forces. As in the core-level studies, the cluster shifts for chloromethane are smaller than those observed for bromomethane clusters, which can be attributed to the larger polarizability of bromine compared to that of chlorine. These results also support the anti-parallel packing as the local structure of these clusters.

Molecular orbital	Character	Cluster shift (eV)	
		CH_3Cl	CH_3Br
2e	localized on halogen	≈ 0.8	≈ 0.9
3a ₁	delocalized over molecule	≈ 0.9	≈ 1.0
1e	localized on CH_3 group	≈ 1.0	≈ 1.1

Table 5.4: CH_3Cl and CH_3Br cluster binding energy shifts with respect to the corresponding molecular lines in the valence region.

The substituent effect in benzene clusters (Paper IV)

In Paper IV, the studies of bromobenzene and chlorobenzene clusters probed by XPS are discussed. The clusters have been produced by adiabatic expansion and different mean sizes have been obtained by varying the carrier gas pressure. The cluster shifts measured for the C 1s, Br 3d and Cl 2p core levels are listed in Tab. 5.5. As in methane-related clusters, it is observed that for

each backing pressure, the halogen-related shifts are significantly smaller than the carbon-related ones. By performing a similar analysis than that described in Sec. 5.1.2, it is inferred that in the most abundant local structure the halogen atoms are mainly surrounded by rings (carbon and hydrogen atoms) and vice versa.

	P_{cg} (bar)	Halogen shift (eV)	Carbon shift (eV)
C₆H₅Cl			
	1.5	0.59	0.79
	2	0.60	0.74
	2.5	0.38	0.66
	3	0.43	0.61
C₆H₅Br			
	1	0.64	0.78
	1.5	0.57	0.76
	2	0.53	0.67
	2.5	0.51	0.60
C₆H₆			
	2		0.50
	2.4		0.66
	3		0.73

Table 5.5: Cluster shifts obtained for chlorobenzene and bromomethane clusters (Paper IV). P_{cg} denotes the helium pressure. The results from benzene series I (Sec. 5.1.1) are also included for comparison.

Chlorine is more electronegative than bromine consequently, the C 1s shift of chlorobenzene would be larger than that of bromobenzene. However, the core-ionized atom is immersed in a polarizable environment. Bromine has more electrons than chlorine to screen the core hole in the carbon atom. This would speak for a larger shift in the bromobenzene case. Ohta et al. have measured core-level spectra of halogen substituted benzene molecules [66]. The C 1s shift of the carbon linked directly to the halogen is 40% larger for chlorobenzene than for bromobenzene [66]. The molecular shifts are affected by the initial charge distribution (which depends on the electronegativity of the halogen atom) and by final state effects (influenced by the polarizability of the halogen atom). Sæthre and co-workers have calculated the contributions of these quantities to the C 1s shifts for haloethenes and haloethanes [67]. They find that the part of the shifts given by initial state effects is larger than that corresponding to final state effects. As expected, the contribution caused by relaxation is larger in compounds containing bromine while the one due to the initial state effects is larger in chlorine substituted molecules [67].

The results obtained for the cluster shifts are compared with those of benzene (Sec. 5.1.1). The uncertainty in the cluster size and intermolecular distances make a direct comparison of the results difficult. However, some general considerations about the differences between the benzene and substituted benzene cluster shifts are outlined. From electrostatic arguments, it is expected that the C 1s shifts of bromobenzene and chlorobenzene clusters are larger than those of benzene clusters, which is observed when the carrier gas pressure is 2–2.5 bar. There seems to be a tendency of larger C 1s shifts in the case of chlorobenzene suggesting that also in the cluster case the initial state effect contribution is more important. However since there are many competing effects influencing the clusters shifts further studies are needed to quantify which property, polarizability or electronegativity, is dominant in this case.

5.2 Heterogeneous molecular clusters: Papers V and VI

The formation process of binary clusters has been studied by means of photoelectron spectroscopy aiming at understanding the changes observed when rare-gas clusters are exposed to polar molecules. These systems are well suited to study inter-atomic and molecular interactions (dipole-induce dipole and dipole-dipole) not present in pure rare-gas clusters. These forces are stronger than the vdW forces and they may alter the host cluster structure. Krypton and argon clusters have been used as host clusters and exposed to chloromethane using the set-up described in Sec. 4.1.2. To get insight in the geometry of these clusters, core-level spectra of the edges Kr 3d, Ar 2p, and Cl 2p have been recorded. There are several differences between the spectra of pure and doped rare-gas clusters, which have been analysed to determine the spatial distribution of the compounds in the clusters. The cluster shifts are indicated in Tab. 5.6.

Cluster	Rg_{bulk} shift (eV)	Rg_{surf} shift (eV)	Cl 2p shift (eV)
Ar	0.96	0.69	
Ar-CH ₃ Cl	1.05	0.80	0.75
Kr	1.12	0.83	
Kr-CH ₃ Cl	1.16	0.93	0.85

Table 5.6: *Comparison between doped and pure rare-gas cluster core-level shifts. Rg_{bulk} and Rg_{surf} denote the rare-gas shift for the bulk and the surface components respectively.*

In both cases, the doped clusters presented larger core-level shifts than the corresponding pure clusters. The cluster shifts are expected to become larger with the cluster size and with the polarizability. An increase in the rare-gas shifts for doped clusters would be mainly caused by changes in the neighbourhood of the rare-gas atoms. Argon and krypton have smaller polarizability

than chloromethane, therefore, the increase in the shifts indicates that chloromethane molecules have rare-gas atoms as nearest neighbours². Since the surface components have changed more than the bulk ones relative to the pure case, it is concluded that most of the molecules are located on the surface of the clusters. For the molecules to migrate into the bulk of the clusters a certain amount of energy is required to weaken the bonds between the rare-gas atoms and to create a hole which contains the molecules in the clusters. Argon has approximately half the cohesive energy of krypton [7] therefore, in the first approximation, more chloromethane molecules are expected to be solvated in argon clusters than in krypton clusters. Changes in the spectral features of doped clusters relative to spectra corresponding to pure argon and krypton clusters seem to indicate some solvation of chloromethane.

The comparison between the value of the shifts of pure chloromethane and that of doped clusters gives also qualitative information about the cluster geometry³. The results obtained for large chloromethane clusters are discussed in Sec. 5.1.2. The observed shifts for doped rare-gas clusters are smaller than those of chloromethane clusters (Tab. 5.3). A smaller value of the Cl $2p$ shift for doped clusters would also indicate that argon atoms are in the vicinity of chloromethane molecules since the polarizabilities of the rare-gas atoms are smaller than that of chloromethane, consequently these atoms induce smaller shifts than chloromethane molecules.

5.3 Metal clusters: Papers VII–XII

Several types of metal clusters have been studied in this Thesis, namely potassium, sodium, lead, copper, silver, tin and bismuth. The clusters have been created with a gas-aggregation source equipped with an oven (K, Na) or a magnetron head (Pb, Cu, Ag, Sn, Bi) to produce the metal vapour (see Fig. 4.2). The motivation for employing two distinct ways of generating the metal vapour is not only the demand for producing clusters of metal atoms with high melting point and/or low vapour pressure, but also that the use of different methods gives the opportunity to experimentally explore to which extent the gas dynamics affect large metal clusters. For example, the analysis of XPS spectra shows that while the clusters obtained with the oven are neutral, the beam generated using the magnetron-based source also contain singly charged clusters.

In order to characterize the electronic structure of the clusters and compare it with that of the corresponding solids, the clusters have been probed by PES.

²This argument is only valid as a first approximation because when the argon/krypton clusters are exposed to chloromethane molecules, it is expected that some rare-gas atoms would evaporate. Consequently, the mean size of doped clusters would be somewhat smaller than that of the original host clusters.

³In this analysis we assume that the differences between the sizes of pure and doped clusters are negligible and the bond distances are comparable for all the systems involved.

Information about the valence band has been obtained and, in some cases, even the outermost core levels have been studied.

5.3.1 Valence band

The valence states of free metal clusters can be investigated using ultraviolet photoelectron spectroscopy (UPS) [2]. For sufficiently high photon energy, the valence spectrum provides a picture of the occupied density of states weighted by the cross section and final state effects [41]. As mentioned in Sec. 4.2.3 a quantitative analysis of the cluster valence spectrum is difficult because the hole is made in the relaxing system and the valence electrons are usually delocalized. However, a qualitative analysis gives direct information about quantities such as the first ionization energy (IE) of the clusters, which can be compared with the work function (W_f) of bulk metals. Furthermore, the IE can be used to obtain an estimation of the cluster size. In addition, the differences between the cluster and solid spectra are indicators of how discrete the valence levels are in the former.

In general, the cluster valence spectra resemble those of the corresponding solids. Table 5.3.1 shows the first ionization potential obtained from the valence spectra. The similarities between the spectral shape and the IE of the clusters and those of the bulk indicate that the cluster have developed a band structure.

	IE (eV)	W_f (eV)
K	2.5	2.3^1 [41]
Na	NA	2.4^1 [41]
Pb	4.3	$3.9\text{--}4.2^2$ [68; 69]
Cu	4.2	4.6^2 [70]
Ag	4.0^*	4.2^2 [71]
Sn	4.4^*	4.4^2 [41]
Bi	NA	4.3^2 [41]

Table 5.7: Comparison between the first ionization potential (IE) of the clusters and the work function (W_f) of the solid. The exponents 1 and 2 indicate that the solid samples are thin films and polycrystalline respectively. The asterisk denotes that the value has not been directly measured but deduced from the experiments together with other considerations. NA indicates that those values have been neither measured nor calculated.

5.3.2 Core levels

The outermost core levels of potassium (3p), sodium (2p), lead (5d), tin (4d), and bismuth (5d) clusters have been measured. Before discussing the results,

the main processes that lead to the observed photoelectron spectra of metallic clusters are briefly summarized. The emission of the core electron due to the absorption of a photon leaves a core hole which interacts with the valence electrons. There are many possible excitations for the valence electrons in a metal. For instance, electron-hole pairs can be induced and they are responsible for the asymmetry of the core line towards higher binding energy. Moreover, collective oscillations of the electrons relative to the positive lattice ions, called plasmons, can be also excited. When the plasmons are created simultaneously with the core hole, they are denominated intrinsic plasmons. Plasmons can also be produced by secondary scattering between the outgoing electrons and the other electrons. In this case, the plasmons are called extrinsic plasmons. There are two types of plasmons: the surface plasmons and the bulk plasmons. They show up in the spectra as satellites shifted in energy from the core lines by an integer of $\hbar\omega_{bp}$ and $\hbar\omega_{sp}$, ω_{bp} and ω_{sp} being the plasmon frequencies corresponding to bulk and surface plasmons [41]. The collisions between the photoelectron and other electrons or lattice ions, in which an unquantized amount of energy is transferred, cause the smooth background observed in the spectra. Figure 5.2 shows a typical core-level spectrum for potassium clusters, in which the plasmon features are indicated.

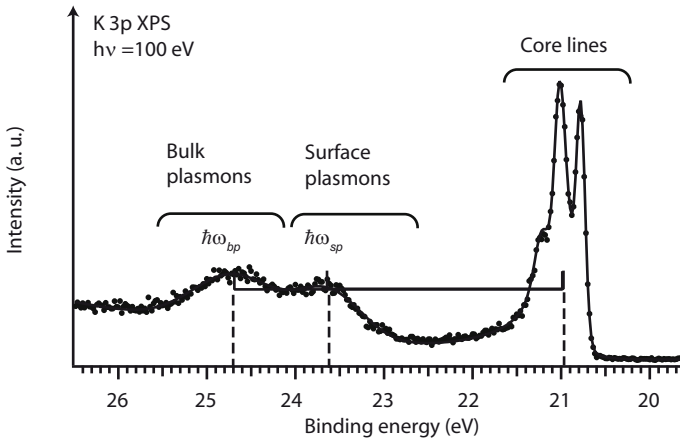


Figure 5.2: K 3p X-ray photoelectron spectra of free K clusters recorded with photons with 100 eV energy. Dots represent experimental data. The fit is shown with a full line.

Because of the similarities between the cluster and bulk spectra the Doniach-Šunjić lineshape (see Sec. 4.2.3) has been used to fit the cluster XPS. However, for bismuth, tin, and lead the cluster features are considerably broader than for sodium and potassium which, to a certain extent, justifies the use of Voigt functions to fit the spectra.

One of the major problems encountered in quantitative analysis of core-level spectra of metallic samples is the determination of the background, and several procedures have been proposed for bulk samples [41]. For example, the straight-line and the Shirley background [72] have been widely used [73].

A more realistic background involving a physical description is obtained employing the Tougaard method [74; 75; 76], which is based on the analysis of energy-loss spectra. Since the application of the Tougaard correction to cluster spectra is mathematically and computationally costly a constant or linear background has been used to fit the cluster spectra.

A precise comparison between the energy positions of the core lines of the cluster and of the solid (cluster-to-solid shift) is rather difficult because the energy scale in the solid spectra are referred to the Fermi level, which is known with limited precision, and not to the vacuum level, as in the cluster case. The cluster-to-solid core-level shifts have been at most ≈ 50 meV for the metal clusters studied in this Thesis, which also supports the conclusion drawn from the analysis of the valence spectra, meaning that the screening mechanism, and then the valence band, in the clusters and in the solid are similar.

Plasmon Satellites

Plasmon satellites have been observed in core-level spectra of potassium clusters (see Fig. 5.2). As mentioned above, surface and bulk plasmons are created simultaneously with the emission of the core electron (intrinsic plasmons) and also by inelastic scattering of the outgoing electrons by the other electrons (extrinsic plasmons). Extrinsic plasmon are thought to be dominant in simple metals. For instance, the contribution of the intrinsic plasmons to the total plasmon excitation in magnesium is $\approx 20\%$ [77]. Consequently, intrinsic plasmons can be neglected when analysing the spectra. The plasmon energies are determined as the difference between the peak position of each plasmon feature and the average of the peak position of the core lines. The values obtained for the plasmon energies ($\hbar\omega_{sp} = 2.6$ and $\hbar\omega_{bp} = 3.7$ eV) are quite similar to the solid ones ($\hbar\omega_{sp} = 2.73$ [78] and $\hbar\omega_{bp} = 3.72$ eV [79]), which is expected since the clusters are rather large, and their spectra resemble the spectrum for solid potassium [80; 81].

Finally, the photon energy dependence of the plasmon satellites has been experimentally investigated for potassium clusters. At higher kinetic energies, the plasmon creation is the main loss mechanism in metals. The ratios between the integrated intensity of core lines and the plasmon satellites are ≈ 1.4 , ≈ 1.7 , and ≈ 1.6 for the measurements performed at 74, 100 and 150 eV photon energies respectively. The electron mean free path increases with photon energy meaning that the energy losses are reduced. Therefore, it can be expected that the ratio between the integrated intensities of the core lines and that of the plasmon satellites increases with photon energy. This tendency is observed in the spectra recorded at 74 and 100 eV photon energy, however further studies are required to confirm it at higher photon energies.

5.3.3 Estimation of the size of metal clusters

The cluster size distribution formed in a gas-aggregation source is broad and depends on many parameters, principally on the time of residence of the clus-

ters in the formation region and on the properties of the cooling gas. In order to make an estimation of the mean size of the clusters, a simple model that relates the cluster first ionization energy to the cluster radius has been used. In a solid metal, the work function is the minimum energy required to remove an electron at the Fermi level. The first ionization energy of a metal cluster approaches the work function of the solid as the cluster size increases. This is reflected by the following formula:

$$IE(Z) = W_f + \frac{e^2(\alpha + Z)}{R + \delta} \quad (5.1)$$

where R is the cluster radius, and Z is the charge state [82]. δ is a size effect coefficient that is a correction added to the cluster radius due to the spill out of the electron density into vacuum [82]. α includes the quantum correction of the bulk work function for a spherical particle [82]. The value of α obtained for simple metal clusters studied within the jellium model is approximately 0.42 [83; 84; 85]. The value of δ strongly depends on the surface structure and the model used [86]. For example, theoretical calculations indicate that δ for potassium lies between 0.76 and 1.67 Å [86].

In an electrostatic description, a large metal cluster can be approximated by a conducting sphere, then α and δ take the values 0.5 [87] and 0 [82] respectively. The classical approximation is appropriate when $\delta \ll R$, that is when the clusters have a sufficiently large size and have fully developed their metallic properties (alkali metal clusters formed by hundred atoms are expected to exhibit a metallic electronic structure [88]). Equation 5.1 is also valid for the core-ionization case, replacing the valence ionization energies by the corresponding core ones, since the core hole is completely screened by the remaining electrons.

Spectra corresponding to metal clusters produced with our source present significant similarities with those of bulk metals indicating that the valence band is formed in the clusters. Therefore, the classical approximation is used, that is $\alpha = 0.5$ and $\delta = 0$. For all cases, the mean size obtained has been thousands of atoms per cluster.

Another estimation of the cluster size can be obtained from the ratio of the integrated intensities of the surface and bulk components in the XPS. The approach presented in Ref. [35] for rare-gas clusters, which assumes that the clusters consist of concentric spherical layers separated by a distance d , has been applied to potassium clusters (Paper VII) giving similar results than those obtained by applying Eq. (5.1).

5.3.4 CVV Auger spectra of alkali metal clusters

Auger spectroscopy is another probe of the occupied part of the valence band and also provides information about the core states (see Sec. 4.2.4). The CVV Auger decay is interesting when applied to alkali metal clusters. Free alkali metal atoms possess only one valence electron, which excludes the possibility

of a normal Auger decay for the outermost core orbital. However, the Auger decay channel is open for these clusters, since each atom contributes with one valence electron. For example, Auger decay has been observed already in sodium dimers where the 3s-derived molecular orbital has two electrons [89]. Auger $L_{2,3}VV$ and $M_{2,3}VV$ spectra have been recorded for sodium and potassium respectively.

As noted in Secs. 4.2.4 and 4.2.5, the Auger spectrum does not reflect the occupation of the valence band in a simple way. However, if effects caused by the localized core hole and the interaction between the two delocalized holes in the valence band are neglected, the Auger electron distribution is proportional to the self-convolution of the density of states (see Eq. (4.4)) [46]. Within this model, it is expected that the lineshape of the CVV Auger feature would be broad with approximately twice the width of the valence band.

In the case of potassium clusters, it has been possible to measure the valence spectrum and, a fair agreement between the calculated width from the $M_{2,3}VV$ Auger spectrum and Eq. (4.4) has been found. For sodium clusters, however, the Auger width was measured to be four times the width of the band, which has been taken from the literature (≈ 3 eV [90]). The excess width in the Auger spectra could be due to other decay mechanisms such as plasmons and shake-up decay. In addition, it is known that there are differences between the measured valence band width and those obtained from calculations [91].

The Auger $M_{2,3}VV$ spectrum of potassium clusters presents a rich satellite structure (see Fig. 5.3), consequently it is further discussed. The normal Auger feature is observed at ≈ 15 eV. There also are two separate humps one on either side on the normal Auger peak. Since the plasmon creation requires energy, the plasmon satellites typically appear on the lower energy side of the Auger peak. They are shifted from the Auger peaks by an integer of $\hbar\omega_{bp}$ and $\hbar\omega_{sp}$ (the bulk and surface plasmons energies respectively) [41]. The band observed at ≈ 12 eV is mainly caused by plasmons, since the surface and bulk plasmon satellites are expected to show up at ≈ 12.3 and ≈ 13.3 eV respectively.

For the higher kinetic energy feature, which is centred approximately at 17 eV, there are two possible assignments. After the creation of a core hole in a free-electron metal, intrinsic plasmons can be excited simultaneously, which can propagate or decay. Under certain circumstances (if the core hole lifetime is sufficiently long [92]), the energy released in the decay of intrinsic plasmons can be transferred to the Auger electron. Those Auger electrons will appear in the spectrum as features shifted towards higher kinetic energy relative to the Auger feature. The shift is given by the plasmon energy as in the case of plasmon-loss satellites. The intensity in this region can be at least partly assigned to a plasmon-gain satellite. Furthermore, the energy position of this satellite would indicate that these plasmons mainly originate from the surface of the clusters.

This higher kinetic energy band could also contain contributions from a shake-up like process which is observed in the core-level photoelectron spec-

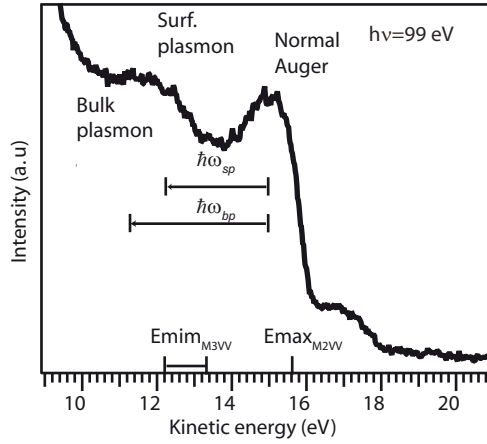


Figure 5.3: $M_{2,3}VV$ Auger spectrum corresponding to free K clusters.

tra of potassium and sodium clusters (Papers VI and VIII). There, it is seen that the core line has a tail towards higher binding energy. In a simple picture, the photoelectron on its way out from the clusters excites a valence electron to an empty state in the conduction band. There are two possible decay channels: spectator and participator Auger decay. In the first, the excited valence electron remains in the conduction band during the Auger decay. In the second, the valence excited electron takes part in the decay where one electron fills the hole and another electron is ejected. The emitted Auger electron from a participator-like channel can have higher kinetic energy than those Auger electrons created in the normal Auger process. Consequently, a part of the signal observed at higher kinetic energy of E_{maxM_2VV} could be due to participator-like decays.

5.3.5 The Born-Haber cycle applied to metal clusters

The Born-Haber cycle is a theoretical approach to obtain atomic core-level binding energies from solid state data by using thermodynamic parameters [41]. When applied to metals, this method relies on the complete screening of the core hole and on the $Z+1$ approximation⁴. A Born-Haber cycle for metals is illustrated in Fig. 5.4. In the first part of the cycle, an atom from a solid element of nuclear charge Z is promoted to the gas phase by giving a quantity of energy equal to the cohesive energy (E_{coh}^Z). Then, this atom is core-ionized producing an ion. The energy required to perform this step is the photoionization energy (E_{core}^{Z-atom}). Within the $Z+1$ approximation, this atom is substituted by an atom with nuclear charge $Z+1$ that is lacking a valence electron. This

⁴The $Z+1$ approximation, also known as “the equivalent core approximation”, assumes that the spatial extension of the core electron is small relative to that of the valence electrons, thus the effect of a core hole can be approximated by an addition of a proton to the nucleus [41].

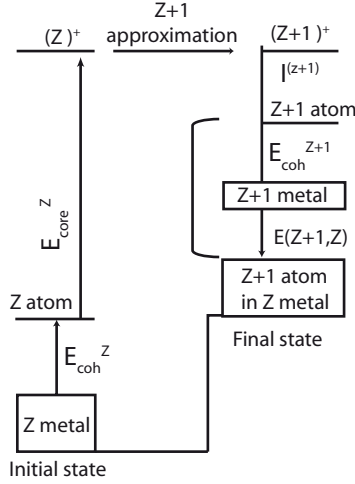


Figure 5.4: Born-Haber cycle to calculate the binding energy in a metal.

$Z+1$ atom is neutralized and gains the ionization energy (I^{Z+1}). Afterwards, it is put back in the Z solid (the original metal) by providing the cohesion energy of the $Z+1$ metal (E_{coh}^{Z+1}). Finally, this $Z+1$ impurity is dissolved in the Z metal and the system gains the solution energy $E(Z+1, Z)$. This state is the same as the final state obtained by core ionizing an atom in the Z metal. Thus, the core-level binding energy of the Z metal $E_{c, Ef}^{Z, metal}$ relative to the Fermi energy (E_f) is:

$$E_{c, Ef}^{Z, metal} = E_c^{Z, atom} - I^{Z+1} + E_{coh}^Z - E_{coh}^{Z+1} - E(Z+1, Z) \quad (5.2)$$

considering that the difference in energy $E_{c, Ef}^{Z, metal} - E_c^{Z, atom}$ is the same for all core levels [41]. Equation (5.2) can be applied to large metal clusters since they possess an electronic structure similar to the corresponding solids. The cluster-to-atom shifts for K, Na, Pb, Sn and Bi obtained experimentally and by using Eq. (5.2) are displayed in Table 5.3.5 (see Paper XII). The agreement between the experimental data and the calculated values is good and validates the underlying assumptions, namely the $Z+1$ approximation and the complete screening picture.

	Δ_{a-c}^{Exp} (eV)	Δ_{a-c}^{BH} (eV)
K	3.8–4.2	4.5–4.6
Na	4.7–4.9	5.1
Pb	3.1–3.4	2.9
Sn	3.4–3.8	3.9
Bi	No atomic data available	3.8

Table 5.8: *Comparison between cluster-to-atom core-level shifts obtained experimentally (Δ_{a-c}^{Exp}) and by applying the Born-Haber cycle (Δ_{a-c}^{BH}).*

6. Summary and outlook

Results concerning molecular and metal clusters based on the analysis of photoelectron and Auger spectra have been presented and several types of problems have been addressed. One of the main objectives of the experimental analysis has been the determination of the cluster local geometry. Suitable packing structures have been proposed employing simple electrostatic considerations. In the case of metal clusters, models from solid state physics have been tested. However, there are many processes that are not clearly understood. The cluster aggregation state is basically unknown. Much has been debated around this point, but there are neither conclusive experiments nor simulations that show the evolution from a liquid to a solid phase with increasing number of atoms. The same can be said about the structure of heterogeneous clusters, little is known about the processes that take place when molecules are deposited on clusters. The electronic structure of large metal clusters resembles that of the solid. However, measurements of standard metallic properties like conductivity have not been performed in clusters. The cluster temperature is an important characteristic, but at the present, it is not possible to measure it on free clusters.

From a broader perspective, it is clear that cluster research has the potential to design new materials with tailor-made properties. The investigation of reactions between molecular clusters can provide understanding of chemical processes that occur in the atmosphere and in biological systems. Even though much progress has been made in cluster science, there is still a long way to go to achieve these objectives. The third generation of synchrotron storage rings have made it possible to apply electron spectroscopy techniques to dilute cluster beams. Concerning core-level related techniques, XPS is especially promising because it has the property of being a site and element sensitive method, meaning that the core-level spectra contain a large amount of information about the geometric and electronic structure of the clusters. In order to extract all this information, theoretical methods and standard procedures to analyse the spectra have to be developed. New powerful experimental techniques are being introduced, like the free electron laser, which will give the opportunity to perform experiments in which a high photon flux is required.

Acknowledgements

I would like to thank my supervisors: Gunnar, Maxim, Olle and Svante for support and encouragement. I also want to thank my colleagues: Andreas, Henrik, Ioana, Marcus, Niklas, Sébastien, Sergey, Torbjörn, and Wandared. I am grateful to Leif Sæthre at the department of Chemistry, Bergen University for interesting discussions. I also thank Sophie Canton at the department of Chemical Physics, Lund University for all the help and support specially with the plan, the measurement and the data analysis of the benzene-related experiments. Since all the work was done at MAX-lab, I am grateful to the MAX-lab staff. I am also extremely grateful to Catta and Lisbet for baking the best kanelbulle in the world, and to Ann, Elisabeth, Helena, and Mats for fixing all the formal papers and helping me starting in Sweden. Many thanks to the lunch table group: Andrius, Johan, Hengameh, Peter, Ola, and Ralf for enjoyable moments during working hours and outside the lab. Finally, thanks to Henrik.

Bibliography

- [1] Israelachvili, J. *Intermolecular and Surface Forces*. Academic Press, 2nd edition, (2002).
- [2] Johnston, R. L. *Atomic and Molecular Clusters*. Taylor & Francis, 1st edition, (2002).
- [3] Edalat, M., Lan, S. S., Pang, F., and Mansoori, G. A. *Int. J. Thermophys.* **1**(2), 177 (1980).
- [4] Raoult, B. and Farges, J. *Rev. Sci. Inst.* **44**(4), 430 (1973).
- [5] Hunter, C. A. and Sanders, J. *J. Am. Chem. Soc.* **112**, 5525 (1990).
- [6] Sygula, A., Fronczek, F., Sygula, R., Rabideau, P., and Olmstead, M. *J. Am. Chem. Soc.* **129**(13), 3842 (2007).
- [7] Lide, D. R., editor. *CRC Handbook of Chemistry and Physics*. CRC-Press, 79th edition, (1998).
- [8] Janda, K. C., Hemminger, J. C., Winn, J. S., Novick, S. E., Harris, S. J., and Klemperer, W. *J. Chem. Phys.* **63**(4), 1419 (1975).
- [9] Henson, B. F., Hartland, G. V., Venturo, V. A., and Felker, P. M. *J. Chem. Phys.* **97**(4), 2189 (1992).
- [10] Arunan, E. and Gutowsky, H. S. *J. Chem. Phys.* **98**(5), 4294 (1993).
- [11] Perera, L. and Amar, F. G. *J. Chem. Phys.* **93**(7), 4884 (1990).
- [12] Otomo, J. and Koda, S. *Chem. Phys.* **242**(2), 241 (1999).
- [13] Lundwall, M., Lindblad, A., Bergersen, H., Rander, T., Öhrwall, G., Tchapyguine, M., Svensson, S., and Björneholm, O. *J. Chem. Phys.* **125**(1), 014305 (2006).
- [14] von Pietrowski, R., von Haeften, K., Laarmann, T., Möller, T., Museur, L., and Kanaev, A. V. *Eur. Phys. J. D* **38**(2), 323 (2006).
- [15] Gough, T. E., Knight, D. G., and Scoles, G. *Chem. Phys. Lett.* **97**(2), 155 (1983).
- [16] Celii, F. and Janda, K. C. *Chem. Rev.* **86**(3), 507 (1986).

- [17] Museur, L., Kanaev, A. V., Castex, M. C., Moussavizadeh, L., von Pietrowski, R., and Möller, T. *Eur. Phys. J. D* **7**(1), 73 (1999).
- [18] Moussavizadeh, L., von Haeften, K., Museur, L., Kanaev, A. V., Castex, M. C., von Pietrowski, R., and Möller, T. *Chem. Phys. Lett.* **305**(5-6), 327 (1999).
- [19] Markovich, G., Perera, L., Berkowitz, M. L., and Cheshnovsky, O. *J. Chem. Phys.* **105**(7), 2675 (1996).
- [20] Weber, J. M., Fabrikant, I. I., Leber, E., Ruf, M. W., and Hotop, H. *Eur. Phys. J. D* **11**(2), 247 (2000).
- [21] Mistro, G. D. and Stace, A. J. *Chem. Phys. Lett.* **196**(1-2), 67 (1992).
- [22] Vach, H. *J. Chem. Phys.* **113**(3), 1097 (2000).
- [23] McNaught, A. D. and Wilkinson, A., editors. *IUPAC Compendium of Chemical Terminology*. International Union of Pure and Applied Chemistry, 2nd edition, (1997).
- [24] Pastor, G. M., Stampfli, P., and Bennemann, K. H. *Phys. Scripta* **38**(4), 623 (1988).
- [25] Kaiser, B. and Rademann, K. *Phys. Rev. Lett.* **69**(22), 3204 (1992).
- [26] Sattler, K., Mühlbach, J., and Recknagel, E. *Phys. Rev. Lett.* **45**(10), 821 (1980).
- [27] Binns, C. *Surf. Sci. Rep.* **44**(1-2), 1 (2001).
- [28] Koperski, J. *Van der Waals Complexes in Supersonic Beams: Laser Spectroscopy of Neutral-Neutral Interactions*. Willey-VCH Verlag GmbH & Co., 1st edition, (2002).
- [29] Baletto, F. and Ferrando, R. *Rev. Mod. Phys.* **77**(1), 371 (2005).
- [30] Peredkov, S. *Free clusters studied by synchrotron-based x-ray spectroscopy: From rare gases to metals*. PhD thesis, Lund University, (2007).
- [31] Tchapyguine, M., Peredkov, S., Svensson, H., Schulz, J., Öhrwall, G., Lundwall, M., Rander, T., Lindblad, A., Bergersen, H., Svensson, S., Gisselbrecht, M., Sorensen, S. L., Gridneva, L., Mårtensson, N., and Björneholm, O. *Rev. Sci. Instr.* **77**(3), 033106 (2006).
- [32] Hagen, O. F. *Z Phys. D* **4**(3), 291 (1987).
- [33] Björneholm, O., Federmann, F., Föcking, F., and Möller, T. *Phys. Rev. Lett.* **74**(15), 3017 (1995).
- [34] Björneholm, O., Federmann, F., Föcking, F., Möller, T., and Stampfli, P. *J. Chem. Phys.* **104**(5), 1846 (1996).

- [35] Tchapyguine, M., Marinho, R., Gisselbrecht, M., Schulz, J., Mårtensson, N., Sorensen, S. L., de Brito, A. N., Feifel, R., Öhrwall, G., Lundwall, M., Svensson, S., and Björneholm, O. *J. Chem. Phys.* **120**(1), 345 (2004).
- [36] Abu-samha, M., Børve, K. J., Sæthre, L. J., Öhrwall, G., Bergersen, H., Rander, T., Björneholm, O., and Tchapyguine, M. *Phys. Chem. Chem. Phys.* **8**, 2473 (2006).
- [37] Bergersen, H., Abu-samha, M., Lindblad, A., Marinho, R., Öhrwall, G., Tchapyguine, M., Børve, K. J., Svensson, S., and Björneholm, O. *J. Chem. Phys.* **125**(18), 184303 (2006).
- [38] Abu-samha, M., Børve, K. J., Harnes, J., and Bergersen, H. *J. Phys. Chem. A* **111**(37), 8903 (2007).
- [39] Jones, G. G. and Taylor, J. W. *J. Chem. Phys.* **68**(4), 1768 (1978).
- [40] Piseri, P., Mazza, T., Bongiorno, G., Lenardi, C., Ravagnan, L., Foglia, F. D., DiFonzo, F., Coreno, M., DeSimone, M., Prince, K. C., and Milani, P. *N. J. Phys.* **8**(8), 136 (2006).
- [41] Hüfner, S. *Photoelectron Spectroscopy*. Springer, 3rd edition, (2003).
- [42] Lindblad, A. *A Treatise on the Geometric and Electronic Structure of Clusters: Investigated by Synchrotron Radiation Based Electron Spectroscopies*. PhD thesis, Uppsala University, (2008).
- [43] Siegbahn, K., Nordling, C., Fahlman, A., Nordberg, R., Hamrin, K., Hedman, J., Johansson, G., Bergmark, T., Karlsson, S.-E., Lindgren, I., and Lindberg, B. *ESCA. Atomic, molecular and solid state structure studied by means of electron spectroscopy*. Almqvist-Wiksells, 1st edition, (1967).
- [44] Sokolowski, E., Nordling, C., and Siegbahn, K. *Phys. Rev.* **110**, 776 (1958).
- [45] Doniach, S. and Sunjić, M. *J. Phys. C Solid State Phys.* **3**(2), 285 (1970).
- [46] Lander, J. J. *Phys. Rev.* **91**(6), 1382 (1953).
- [47] Nolting, W. *Z Phys. B* **80**(1), 73 (1990).
- [48] Cooper, J. and Zare, R. N. *J. Chem. Phys.* **48**(2), 942 (1968).
- [49] Dill, D. *J. Chem. Phys.* **65**(3), 1130 (1976).
- [50] Bässler, M., Forsell, J. O., Björneholm, O., Feifel, R., Jurvansuu, M., Aksela, S., Sundin, S., Sorensen, S. L., Nyholm, R., Ausmees, A., and Svensson, S. *J. Electron Spectrosc. Relat. Phenom.* **101-103**(1), 953 (2004).

- [51] Wiedemann, H. *Particle Accelerator Physics I*. Springer, 2nd edition, (1998).
- [52] Aksela, S., Kivimäki, A., Nyholm, R., and Svensson, S. In *Proceedings of the 4th international conference on synchrotron radiation instrumentation*, volume 63, 1252. AIP, (1992).
- [53] Bartell, L. S. and Xu, S. *J. Phys. Chem.* **95**, 8939 (1991).
- [54] Xu, S. and Bartell, L. S. *J. Phys. Chem.* **95**, 13544 (1993).
- [55] Beniere, F. M., Boutin, A., Simon, J. M., Fuchs, A. H., de Feraudy, M. F., and Torchet, G. *J. Phys. Chem.* **97**(40), 10472 (1993).
- [56] Ågren, H. *J. Chem. Phys.* **79**, 587 (1983).
- [57] Riga, J., Pireaux, J., and Verbist, J. *Mol. Phys.* **34**(1), 131 (1977).
- [58] Nordgren, J., Selander, L., Pettersson, L., Brammer, R., Bäckström, M., and Nordling, C. *Phys. Scripta* **27**, 169 (1983).
- [59] Heenan, R. K., Valente, E. J., and Bartell, L. S. *J. Chem. Phys.* **78**(1), 243 (1983).
- [60] Valente, E. J. and Bartell, L. S. *J. Chem. Phys.* **80**(4), 14517 (1984).
- [61] Demuth, J. E. and Eastman, D. E. *Phys. Rev. Lett.* **32**, 1123 (1974).
- [62] Gilberg, E., Hanus, M. J., and Foltz, B. *Japanese J. Appl. Phys.* **17**(17–2), 101 (1978).
- [63] Tegeler, E., Wiech, E., and Faessler, A. *J. Appl. Phys. B* **13**, 4771 (1980).
- [64] Harnes, J., Abu-samha, M., Winkler, M., Bergersen, H., Sæthre, L. J., and Børve, K. J. *J. Electron Spectrosc. Relat. Phenom.* **10.1016/j.elspec.2008.07.011** (2008).
- [65] Kimura, K., Katasumata, S., Achiba, Y., Yamazaki, T., and Iwata, S. *Handbook of HeI photoelectron spectra of fundamental organic molecules : ionization energies, ab initio assignments, and valence electronic structure for 200 molecules*. Japan Scientific Society Press, 1st edition, (1981).
- [66] Ohta, T., Fujikawa, T., and Kuroda, H. *Bull. Chem. Soc. Jpn.* **48**, 2017 (1975).
- [67] Sæthre, L. J., Siggel, M. R. F., and Thomas, T. D. *J. Electron Spectrosc. Relat. Phenom.* **49**(2), 119 (1989).
- [68] Bancroft, G. M., Gudat, W., and Eastman, D. E. *J. Electron Spectros. Relat. Phenom.* **10**(4), 407 (1977).

- [69] Gürtler, K. and Jacobi, K. *Surf. Sci.* **134**(2), 309 (1983).
- [70] Eastman, D. E. *Phys. Rev. B* **2**(1), 1 (1970).
- [71] Barrie, A. and Christensen, N. E. *Phys. Rev. B* **14**(6), 2442 (1976).
- [72] Shirley, D. A. *Phys. Rev. B* **5**(12), 4709 (1972).
- [73] Seah, M. P. *Practical Surface Analysis*, volume 1. Wiley, 1st edition, (1990).
- [74] Tougaard, S. *Surf. Interface Anal.* **11**(9), 453 (1988).
- [75] Tougaard, S. *J. Electron Spectrosc. Relat. Phenom.* **52**, 243 (1990).
- [76] Simonsen, A. C., Yubero, F., and Tougaard, S. *Surf. Sci.* **436**, 149 (1999).
- [77] van Attekum, P. M. T. M. and Trooster, J. M. *Phys. Rev. B* **20**(6), 2335 (1979).
- [78] Tsuei, K. D., Plummer, E. W., Liebsch, A., Pehlke, E., Kempa, K., and Bakshi, P. *Surf. Sci.* **247**(2-3), 302 (1991).
- [79] Raether, H. *Excitation of Plasmons and Interband Transitions by Electrons*, volume 88 of *Springer Tracts in Modern Physics*. Springer, 1 st. edition, (1980).
- [80] Wertheim, G. K., Riffe, D. M., Smith, N. V., and Citrin, P. H. *Phys. Rev. B* **46**(4), 1955 (1992).
- [81] Wertheim, G. K. and Riffe, D. M. *Phys. Rev. B* **52**(20), 14906 (1995).
- [82] Hoffmann, M. A., Wrigge, G., and v. Issendorff, B. *Phys. Rev. B* **66**(4), 041404 (2002).
- [83] Seidl, M. and Brack, M. *Ann. Phys.* **245**(2), 275 (1996).
- [84] Seidl, M., Perdew, J. P., Brajczewska, M., and Fiolhais, C. *Phys. Rev. B* **55**(19), 13288 (1997).
- [85] Seidl, M., Perdew, J. P., Brajczewska, M., and Fiolhais, C. *J. Chem. Phys.* **108**(19), 8182 (1998).
- [86] Kiejna, A. *Phys. Rev. B* **47**(12), 7361 (1993).
- [87] Brack, M. *Rev. Mod. Phys.* **65**(3), 677 (1993).
- [88] Wertheim, G. K., DiCenzo, S. B., and Buchanan, D. N. E. *Phys. Rev. B* **33**(8), 5384 (1986).
- [89] Rander, T., Schulz, J., Huttula, M., Makinen, A., Tchapyguine, M., Svensson, S., Öhrwall, G., Björneholm, O., Aksela, S., and Aksela, H. *Phys. Rev. A* **75**(3), 032510 (2007).

- [90] Höchst, H., Steiner, P., and Hüfner, S. *Z Phys. B* **30**(2), 145 (1978).
- [91] Yasuhara, H., Yoshinaga, S., and Higuchi, M. *Phys. Rev. Lett.* **83**(16), 3250 (1999).
- [92] Gunnarsson, O., Schönhammer, F., Fuggle, J. C., and Lässer, R. *Phys. Rev. B* **23**(9), 4350 (1981).

Acta Universitatis Upsaliensis

*Digital Comprehensive Summaries of Uppsala Dissertations
from the Faculty of Science and Technology 561*

Editor: The Dean of the Faculty of Science and Technology

A doctoral dissertation from the Faculty of Science and Technology, Uppsala University, is usually a summary of a number of papers. A few copies of the complete dissertation are kept at major Swedish research libraries, while the summary alone is distributed internationally through the series Digital Comprehensive Summaries of Uppsala Dissertations from the Faculty of Science and Technology. (Prior to January, 2005, the series was published under the title "Comprehensive Summaries of Uppsala Dissertations from the Faculty of Science and Technology".)



ACTA
UNIVERSITATIS
UPSALIENSIS
UPPSALA
2008

Distribution: publications.uu.se
urn:nbn:se:uu:diva-9323